# A Review Study on the Modeling of High-Temperature Solar Thermal Collector Systems

Hachicha, A.A.[1, *], Yousef, B.[1], Said, Z.[1], Rodríguez, I.[2]

[1]University of Sharjah, College of Engineering, Sustainable and Renewable Energy Engineering Department, Sharjah, P. O. Box 27272, UAE.
[2] Heat Engines Department, Universitat Politècnica de Catalunya-BarcelonaTech. Spain.

[*]Corresponding author: ahachicha@sharjah.ac.ae; ahmedamine.hachicha@yahoo.fr

## Abstract

Concentrated solar power technologies are gaining more attention in the last two decades in order to replace the conventional power technologies and reduce their environmental impact. Among the developed concentrating technologies, parabolic trough solar collector and solar tower are the most mature and dominant technologies. As part of the continuous development of these technologies, significant efforts have been deployed to predict and improve their performance, and therefore reduce their cost and make them more competitive. In this context, numerous analytical and numerical studies have been developed and presented in the literature. This review aims to summarize the state-of-the-art modeling approaches used to simulate, predict and evaluate the optical, thermal and dynamic performance of high-temperature solar thermal collectors. The review includes the different analytical and ray tracing models used to determine the non-uniform flux on the receiver aperture. Energy balance models are also presented as simple and easy computational models suitable to predict the thermal performance at a reasonable time and computational cost, whereas Computational Fluid Dynamic models are more convenient to study the details of the coupled fluid flow and heat transfer in the internal and external flow. The review also includes dynamic models such as the lumped capacitance models which are used to simulate the dynamic characteristics of the heat transfer fluid and interaction with the solar receiver under transient conditions. The dynamic behavior of the whole solar plant using different codes is examined. Furthermore, different features and capabilities of those approaches are also analyzed and compared. Finally, the use of numerical modeling in the development of new designs and assessment of the use of nanofluids is discussed. In summary, this work presents a comprehensive review of the existing numerical models and could serve as a guideline to develop new models for future trends in concentrating solar technologies.

## Graphical Abstract

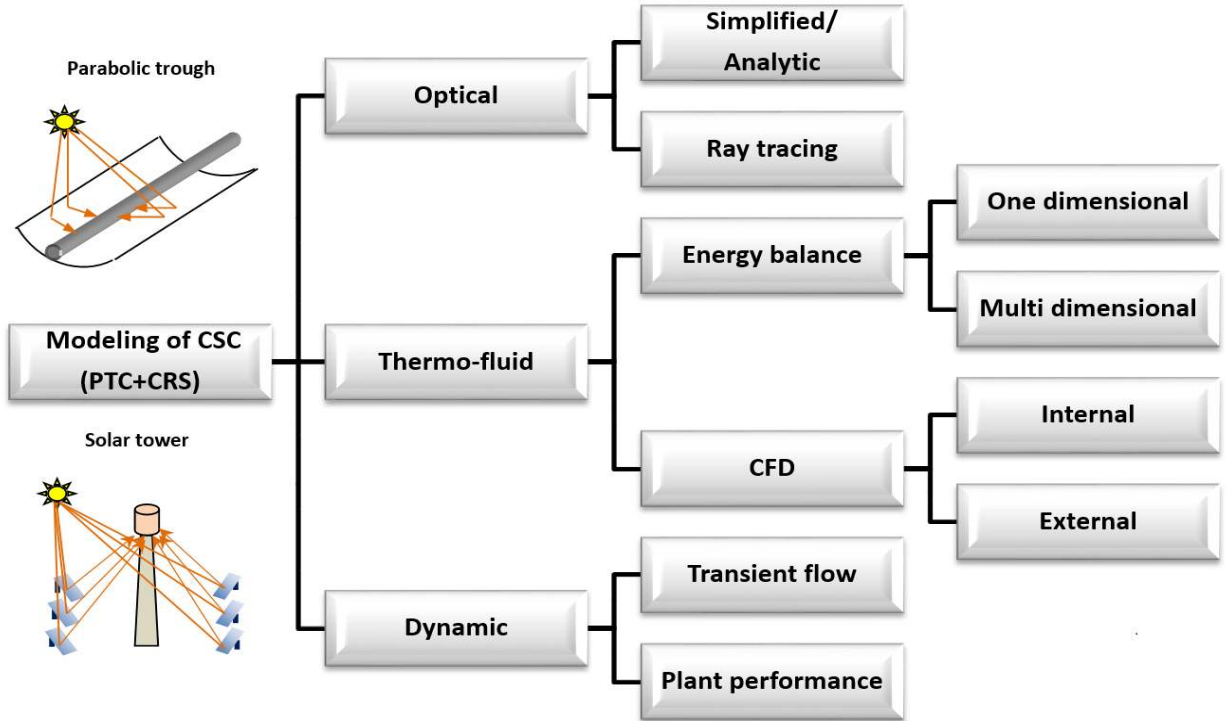

**Highlights:**

- Modeling approaches used for concentrating solar collectors are reviewed.
- Optical modeling is essential to determine the solar flux distribution.
- Computational fluid dynamic models are more convenient for detailed flow analysis.
- Dynamic models are used for transient and power plant simulations.
- New trends in performance enhancement using new designs and nanofluids are discussed.

**Keywords:** Concentrating solar power; Optical models; Thermo-fluid models; Dynamic models; Novel designs; Nanofluids
**Word count:** 10561

**Declarations of interest:** none

List of Abbreviations

| | |
|---|---|
| CFD | Computational fluid dynamics |
| CRS | Central receiver systems |
| CSC | Concentrating solar collectors |
| CSP | Concentrated solar power |
| CV | Control volume |
| DES | Detached eddy simulations |
| DNI | Direct normal irradiance |
| DNS | Direct Numerical Simulation |
| DSG | Direct steam generation |
| FVM | Finite volume method |
| HCE | Heat collector element |
| HTF | Heat transfer fluid |
| LBM | Lattice Boltzmann method |
| LEC | Levelized electricity cost |
| LES | Large eddy simulations |
| LFR | Linear Fresnel reflector |
| MCRT | Monte Carlo Ray tracing |
| PEC | Performance evaluation criterion |
| PSO | Particle swarm optimization |
| PTC | Parabolic trough collector |
| RANS | Reynolds Averaged Navier-Stokes |

## 1. Introduction

In the current context of increasing energy demand and related environmental concerns, solar energy appears to be one of the most efficient and effective solutions in the sustainable development [1]. Additionally, solar energy is the most abundant renewable source of energy available on earth in both direct and indirect forms. Only 0.1% of this energy can be used to generate four times the total world consumption capacity at an efficiency of 10% [2]. In practice, solar energy can be harnessed in two different ways: direct electricity conversion using photovoltaic technology, or indirectly through thermal conversion using solar thermal energy systems. In solar thermal applications, the incoming radiation is absorbed by a solar collector as heat and then transferred to the heat transfer fluid (HTF). Solar collectors can be classified into two main categories: low-temperature for non-concentrating collectors and high-temperature for concentrating collectors.

Concentrated solar power (CSP) technologies are emerging solutions that concentrate the solar radiation to produce high-temperature thermal energy. Nowadays, CSP systems are used in various applications such as heating, process heat, chemical process, and mostly in electricity production. CSP has the advantage of promising cost-effective investment, as well as the easy coupling with storage solutions and other renewable energy sources [3, 4]. Among the different technologies that can be used in the solar field of CSP plants, both parabolic trough collectors and solar towers are occupying an important market position due to their lower operating costs, higher efficiency and flexibility to scale up in large power plants [5]. According to these advantages, it is estimated that CSP plants could produce as much as 7% of the world global electricity by 2030, and 25% by 2050 [6]. Recently, new CSP projects in Australia and Dubai announced a record low tariffs of electricity below 0.07 USD per kWh which could mark the commercial breakthrough of CSP [7].

In order to compete with conventional sources of energy, CSP technologies have experienced significant research and development efforts [8, 9]. To this end, various challenges are addressed to develop new designs, materials, heat transfer fluids and, processes to increase the thermal efficiency and reliability over multiple thermal cycles. In this context, the modeling of these systems is a powerful tool to predict the complex system behavior and make these technologies more mature technically and economically. Several modeling approaches are presented in the literature to analyze, optimize, and enhance the performances of concentrating solar collectors (CSCs). These models studied the optical and thermal performances under operating conditions, as well as the wind effect and dynamic evolution under variable external conditions. Although some authors have reviewed new designs [10], materials [11], and heat transfer fluids (HTF) [12] employed for CSC technologies, the review of numerical modeling approaches used to simulate such systems is limited.

Up to the knowledge of the authors, there is only one review study [13] that discussed the modeling and simulation developed to characterize the performance of parabolic trough technology. However, there is a lack of a comprehensive study that summarizes the state-of-the-art modeling approaches used to investigate the performance of the dominant CSP technologies (parabolic trough and solar tower). Furthermore, little attention has been given to compare the attributes and applicability of such approaches in the development of new designs and processes.

This review aims to examine the numerical modeling approaches used in the recent literature to simulate the main two commercial CSP technologies: parabolic trough and central receiver systems (CRS). A comparison between the different models used is presented and the attribution of each model is also discussed. Furthermore, the use of numerical modeling in the development of new designs and assessment of the use of nanofluids is examined to suggest the future trends in CSP technologies.

## 2. Overview of high-temperature solar collectors

Currently CSP technologies have gained a great interest in their applicability and economic feasibility for electricity generation. CSP technologies are mainly divided into two categories according to the way they are focusing the solar radiation: i) line-focusing systems and ii) point focusing systems [14]. In the

former, the system tracks the sun in one direction (one-axis tracking) such as the case of parabolic trough collectors (PTC) and linear Fresnel reflector (LFR), whereas in the latter the sun tracking occurs in two axes, as in the case of central receiver systems or parabolic dishes (see Figure 1). Parabolic trough solar collectors and central receiver systems are the most developed CSP technologies occupying important positions in the market due to higher efficiencies and lower operating costs [9].

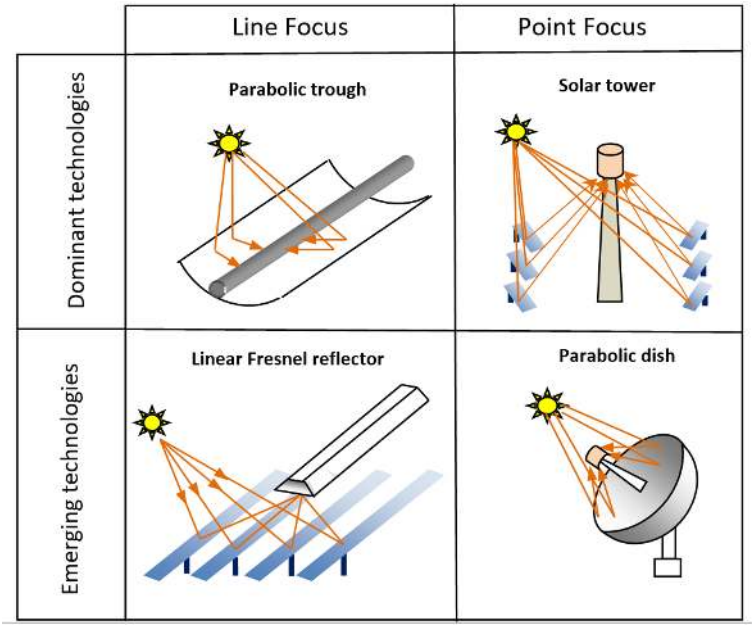


**Figure 1.** Classification of concentrated solar power technologies.

Parabolic trough solar collector is a line focus technology that uses a parabolic reflector to concentrate the beam radiation on the collector axis. The governing equation of a PTC profile in the (x,y) coordinates as a function of the focal length f of the parabola can be expressed as

$$x^2 = 4fy \quad (1)$$

An evacuated receiver is placed on this focal line to absorb the concentrated solar energy and convert it into thermal energy that will be transferred through a heat transfer fluid to the thermodynamic cycle. The receiver consists of a metal tube coated with selective layers and a glass envelope to minimize the heat losses. Synthetic thermal oil is commonly used as HTF in PTC solar plants whereas other HTFs such as water/steam, molten salts and pressurized gases are emerging [15, 16]. A one axis tracking system is used to follow the sun throughout the day and maximize the radiation collection. The continuous development and the reduced cost made this technology more attractive to other applications such as industrial process heat, desalination, domestic water heating and space heating [13, 17].

Solar tower or also called central receiver systems is a point focus technology that uses several sun-tracking mirrors (heliostats) to concentrate the sunlight onto a fixed receiver located at the top of the tower. This point-focused technology uses dual-axis tracking system to track the sun for each heliostat, and a working fluid is circulated on the receiver to absorb the concentrated solar radiation. Solar tower can achieve higher temperature levels than parabolic trough because of its higher concentration ratio. Depending on the design of the tower, different heat transfer fluids such as water/steam, air or molten salt can also be used with this technology [18, 19].

## 3. Review of different design and modeling approaches

With the continuous advances in numerical methods and computing power, numerical modeling and simulation of high-temperature solar collectors have played an important role in the prediction, optimization, and improvement of the global performances of such devices. Moreover, a proper model

can provide a wealth of information on CSC performance without the need to build expensive and time-consuming facilities.

Mathematical models of CSC started in the early 90s with the development of CSP technologies (see for instance [20, 21]). These early models were developed for both the operation of the CSP plant [19] and the modeling of the parabolic trough [17], and were upgraded in the following years. These models can be classified into three main modeling areas: i) Optical models which describe the optical characteristics of the concentrator and solar receiver, ii) thermo-fluid models which estimate the useful gain and thermal losses from the solar receiver as well as the thermal performance under different conditions considering the wind effects, and iii) Dynamic models that simulate the transient behavior of the solar receiver and evaluate the overall dynamic performance of the solar plants. Figure 2 shows the different model categories investigated in this paper.

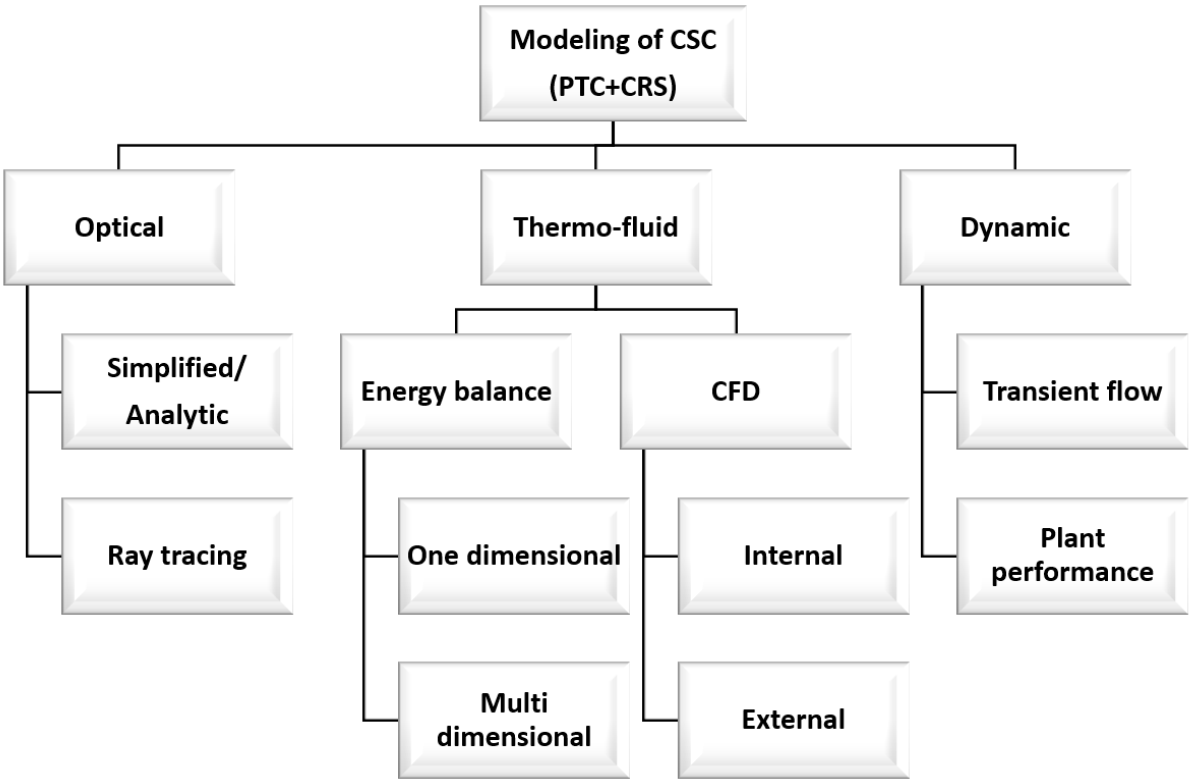


**Figure 2.** Different model categories investigated in this paper.

### 3.1. Optical modeling

Concentrating technologies employ a concentration system which is designed to increase the solar flux reaching the solar receiver. This process of photo-thermal conversion is characterized by a main parameter, so-called concentration ratio. This parameter is generally defined in two different ways: in terms of the radiation that reaches the receiver with respect to the incident radiation, or geometrically as the ratio of the collector aperture to the absorber area. This last one is also called geometric concentration ratio.

In order to estimate the absorbed solar radiation on the CSCs, various optical models have been developed in the literature with different levels of complexity. The outcome of these optical models is necessary to evaluate, optimize and predict the optical characteristics and performance of the CSCs.

Simplified optical models, such as those proposed by Duffie and Beckman [20], assume a uniform solar flux around the receiver and depends mainly on the optical characteristics of the different components. The absorbed radiation per unit of aperture is given as

$$S = DNI\ \rho(\gamma\tau\alpha)_n K \quad (2)$$

Where $DNI$ is the direct normal irradiance, ρ is the specular reflectance of the concentrator, τ is the transmittance of the glass, α is the absorbance of the absorber, γ is the intercept factor and K is the incidence angle modifier. The optical properties are normally function of the incidence angle, and can be evaluated at a normal incident angle while the deviation to the actual incident angle should be considered in the so-called incidence angle modifier. The latter is defined as the ratio of the efficiency at a given angle of incidence (θ) to the efficiency at normal incidence. As it depends on the geometry and the optics of the system, functions for this parameter for different concentrators have been reported in the literature (see Table 1).

Table 1. Incidence angle modifier for different concentrators.

| Concentrator | Incidence angle modifier | Reference |
|---|---|---|
| LS-2 | $K(\theta)_{vacuum} = \cos(\theta) - 0.000884\theta - 5.369 \times 10^{-5}\theta^2$<br>$K(\theta)_{bare} = \cos(\theta) - 0.0003512\theta - 3.3137 \times 10^{-5}\theta^2$ | [21] |
| LS-3 | $K(\theta)_{25m} = 1 - 0.00188\theta - 1.49206 \times 10^{4}\theta^2$<br>$K(\theta)_{50m} = 1 - 0.00362\theta - 1.32337 \times 10^{-4}\theta^2$ | [22] |
| Eurotrough | $K(\theta)_{vacuum} = \cos(\theta) - 5.25097 \times 10^{-4}\theta - 2.958621 \times 10^{-5}\theta^2$ | [23, 24] |

The intercept factor is the fraction of the reflected radiation reaching the receiver surface and includes all optical errors, i.e. receiver shadowing, tracking errors, dirt, etc. The simplified model proposed by Duffie and Beckman [20] can be applied to all concentrators and configurations without taking into consideration the variation of the solar distribution with the position.

However, in practice, concentrating solar receivers are subject to non-uniform solar flux, which may affect the optical characteristics and temperature distribution around the receiver. Therefore, many authors have investigated the solar flux distribution in CSCs [25, 26].

According to the state of the art, several published works have been devoted to study the heat flux distribution and optical performances of PTCs, either by considering the non-uniform heat flux distribution [27], by means of analytical solutions [28] and also taking into account focus and tracking errors [29]. The schematic of the involved components in the optical modeling of PTC is shown in Figure 3.

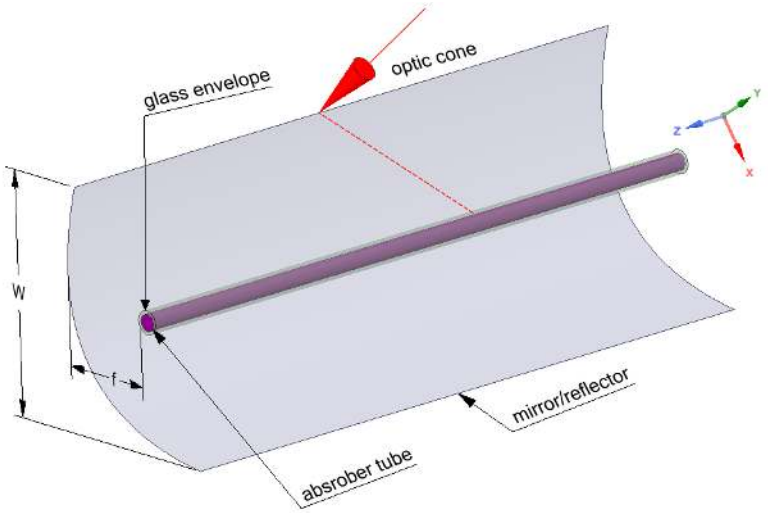


**Figure 3**. Schematic of optical modeling of PTC.

Initially, the majority of proposed models used mathematical/statistical approaches [30, 31] to evaluate the intercept factor and study the effect of the different optical errors that may occur; such as tracking, displacement, mirror specularity, and slope errors.

Jeter et al. [32] presented a pioneer analytical model to evaluate the concentrated radiant flux and optical characteristics of a PTC considering the imperfections of the different optical properties. These kinds of models are based on convolution approaches and require complicated mathematical derivations but less computational time.

Recent published works are based on the statistical Monte Carlo Ray tracing (MCRT) methods which are more flexible in modeling non-ideal optics compared to the simplified models [25, 33]. The principle of ray tracing methods is to randomly generate a large number of rays/photons, and track their paths from one surface to another considering the sun shape and optical effects [26]. The rays/photons are then counted through their hitting positions on the CSC components. Consequently, the non-uniform distribution of the absorbed solar radiation on the absorber/glass tube can be determined and eventually coupled to a thermal model. The optical efficiency of the PTC system is then calculated as the ratio between the statistical absorbed solar radiation to the total solar radiation received on the collector aperture.

He et al. [34] developed a MCRT model to track the photons in their pathways from the parabola to the absorber tube considering the sun shape. The model was validated with the analytical results of Jeter [32] and integrated into a Computational Fluid Dynamics (CFD) model. Cheng et al. [35, 36] proposed a home-made unified code based on MCRT model to simulate different types of concentrating solar collectors. They showed that the solar flux distribution is symmetrical in the cross section and non-uniform in the azimuthal direction. The model is later coupled to a 3D finite volume method (FVM) to study the relation between the geometric parameters of the reflector and the focal shape on the performance of the PTC [37]. The same model [38] is coupled with a population-based particle swarm optimization (PSO) algorithm to optimize the geometric characteristics. Although the computational cost is quite expensive, the model was proven to be feasible and give accurate results.

Liang et al. [25] compared MCRT model with two ray tracing models combined with FVM. They observed that the runtime and computational effort for the proposed modified ray tracing models were improved by 40 to 60%.

Hachicha et al. [39] developed a novel optical model based on a combination of finite volume and ray tracing methods to project the sun shape on the absorber surface. A numerical-geometrical methodology

is applied to discretize the PTC domain and optic cone into control volume and control angles, respectively. A typical solar flux distribution around an LS3 parabolic trough is shown in Figure 4.

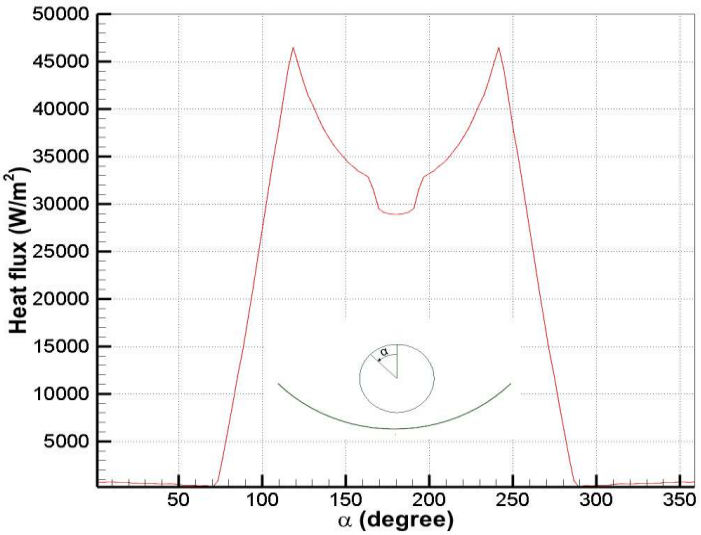


**Figure 4.** Typical flux distribution around an LS3 parabolic trough [40].

MCRT method has not only been used for studying the effects of geometrical parameters, such as aperture width, focal length, and absorber diameter, on the optical performance of a PTC [41-43], but it has also been useful for another kind of concentrator devices such as cavity receivers [44] and parabolic dishes [45].

In the particular case of central receiver systems, the optical modeling is an important step to determine the solar flux concentration through a tower-heliostat field system, and optimize the design of the CRS power plants [26]. One of the main purposes of optical modeling in CRS is to determine the image of the solar disk on the focal plane considering the different defects encountered in the solar facility. The optical modeling of solar tower involves the investigation of optical properties of reflector materials, the heliostat geometry, tracking algorithm, and receiver influence on the concentration and energy yield. The main parameters that may affect the optical efficiency of CRS systems are: cosine effect, shading effect, blocking, atmospheric attenuation and receiver spillage [19]. The optical modeling includes different parameters of both heliostat and receiver geometry.

The optical analysis in CRS is essential in both pre-design and design phases, and can be useful to determine a cost-optimized solution for the solar field layout. In Figure 5, a typical solar flux density observed in a multi-tube cavity receiver is shown. The solar flux distribution in this kind of systems exhibits a non-uniform behavior. Due to the point-focusing system, the maximum flux is measured at the center of the cavity to decrease towards the margin. This uneven distribution affects the solar flux received by each tube, the larger irradiation being in the middle part to decrease towards the tubes end. By using the kind of analysis shown in Figure 5, it is possible to detect problems with the focus strategy. For instance, by performing the optical analysis of the cavity receiver, Qiu, Y et al. [46] recommended the use of a multi-point focus strategy instead of the traditional one-point strategy in order to make more homogenous the solar flux which leads to an increase of the optical efficiency of the system.

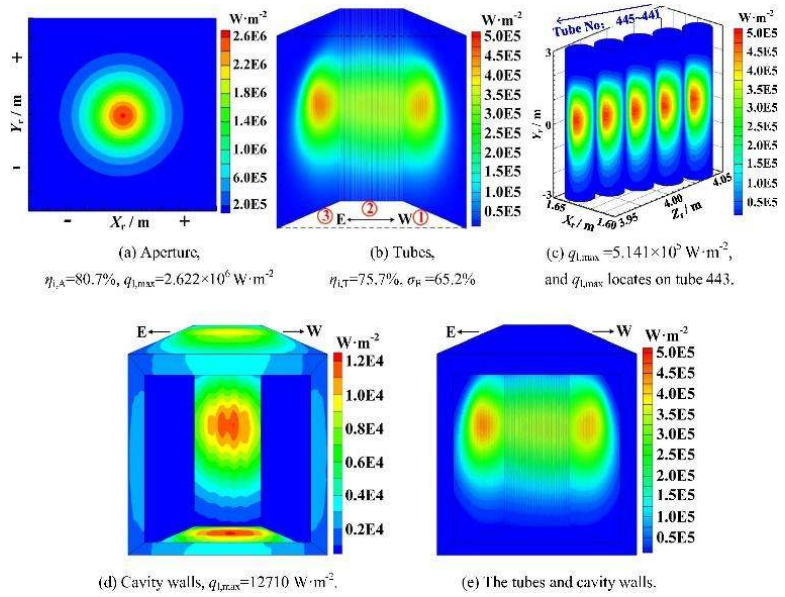


**Figure 5.** Typical solar flux distributions in a multi-tube cavity receiver [46]. (License number: 4492630801860)

Moreover, the prediction of the flux density distribution on the heliostat field with high accuracy is essential in the design phase of the heliostat field [47, 48] and is commonly used for the optimization of the solar field layout for CSP plants such as in PS10 [49] or DAHAN [50, 51]. The most important strategies for optical modeling of CRS are divided in two categories, the flux distribution prediction and the heliostat field optimization, as shown in Figure 6. The first category refers to the codes and models capable of accurately simulating the solar flux distribution reaching the receiver from the heliostat field. The second category includes the parametric analysis and optimization of the heliostat field which may help to reduce the energy costs and improve the heliostat field layout.

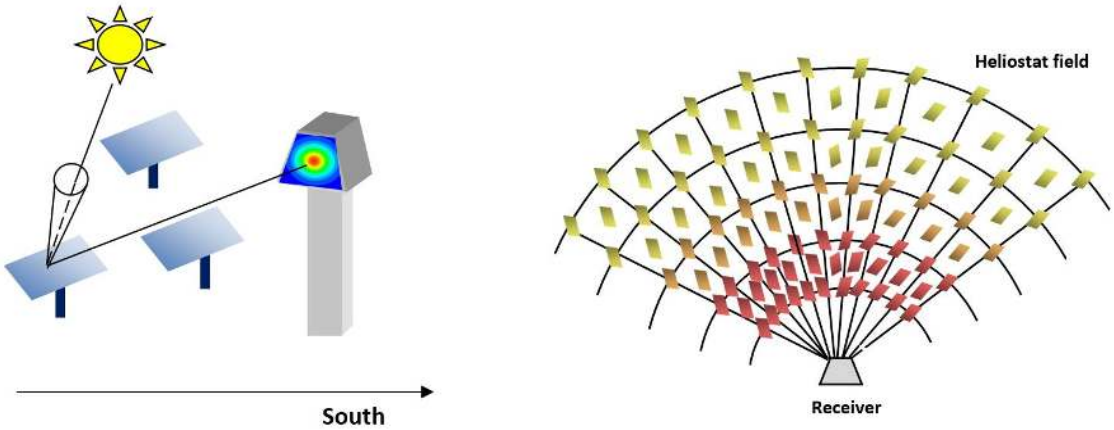


**Figure 6.** Most important strategies for optical modeling of CRS: (left) flux distribution prediction (right) heliostat field optimization

Besides the great importance in modeling the complex solar field in CRSs and its optical performance, CRS optical models may allow the integration with optimization algorithms and overall plant models.
In the literature, several codes and algorithms for the optical modeling of CRS systems are presented in [26, 52, 53]. These codes can be classified into three groups:
i) Codes that use statistical approaches based on convolution/expansion techniques or MCRT like HELIOS [54], MIRVAL [55], FIAT LUX [56] and SolTrace [57], STRAL [47], TONATIUH [58] and others.

ii) Codes that use simplified optical models to reduce calculation time with an emphasis on the design and optimization of the whole CRS system like the University of Houston Codes (UHC), (WIN)DELSOL [59] and HFLCAL [60]
iii) Codes that use a detailed analysis of the optical performance with an optimization of the overall system like SCT [61] or SENSOL [62] or Raytrace3D [53].
These codes include different modules and functionalities that can be used to study heliostat field layout, heliostat tracking and representation of both facet and receiver geometry. In terms of accuracy, the first and third categories are more accurate for predicting the flux distribution in the heliostat-receiver system, while the second one is more recommended for techno-economic assessment of the CRS technology. A comparison between three codes from each category is shown in table 2.

Table 2. Comparison between different optical codes: DELSOL, SolTrace and Raytrace3D. Adapted from [53].

| **Main features** | **DELSOL** | **SolTrace** | **Raytrace3D** |
|---|---|---|---|
| Type of tool | optimization | Performance analysis | Performance analysis optimization |
| Considered subsystem | overall plant | optical subsystem | optical subsystem |
| Calculation method | Hermite polynomial expansion/convolution | MCRT | MCRT |
| Contribution of each loss | Yes | No | Yes |
| Accuracy | Increases with field size | Accurate for one heliostat | Accurate for one facet of a heliostat |
| Optimized components | Heliostat boundary, field layout, tower height, receiver size, storage capacity | Not available | field layout (tower height, heliostat geometry, facet curvature, receiver size) |
| Optimization criteria | Cost criteria with optional flux/land constraints | Not available | geometrical concentration, flux density, (plant energy production, LEC) |

### 3.2. Thermo-fluid modeling

The thermo-fluid modeling of high-temperature solar thermal systems is essential to simulate, control and optimize the thermal performance of concentrating receiver collectors. Two main approaches are developed in the literature for the analysis and prediction of thermo-fluid characteristics of concentrating solar collectors. The first approach is commonly used in the prediction of the thermal losses and temperature variation without solving the fluid dynamics, and it is based on energy balance [63, 64]. The second approach provides more details on the fluid flow behavior by solving the governing mathematical equations using CFD [65, 66].

#### 3.2.1. Energy balance models

Energy balance models focus on the prediction of thermal performances of the CSCs and their receivers. They usually include the optical losses and thermal losses, together with the boundary conditions of the concentrator, i.e. weather conditions which include direct normal irradiation (DNI), ambient temperature, wind velocity, sky temperature, etc., and receiver geometrical conditions. The governing energy balance equation applied to a control volume (CV) can be expressed in a general form as

$$Q - W = \int_{CV} \frac{\partial(\rho e)}{\partial t} dV + \int_{CS} \rho e \vec{V} \cdot \vec{n}\ dA \quad (3)$$

where e is the total energy rate within the CV, Q is the rate of heat added to CV and W is the net of work done on the CV. This equation needs to be applied over each part of the CSC and coupled with the optical model in order to determine the useful energy gains, thermal losses and optical losses. In order to simplify the analysis, the heat losses coefficient concept can be used to include the different losses (by radiation and convection, mainly) between the solar receiver and the surroundings[20, 67]. The useful energy gains equation under such conditions is expressed as

$$Q_u = DNI\eta_o A_a - A_r U_L (T_r - T_a) \quad (4)$$

In the above equation, $A_a$ represents the solar field aperture, $A_r$ is the receiver area, and $T_r$ and $T_a$ are the receiver and ambient temperature, respectively. In a similar way to a flat-plate collector, the above equation can be also expressed in terms of the fluid temperature at the inlet of the concentrator $T_i$ as

$$Qu = F_R[DNI\eta_o A_a - A_r U_L (T_i - T_a)] \quad (5)$$

Where $F_R$ is the heat removal factor given as

$$F_R = \frac{\dot{m}c_p}{A_r U_L}(1 - \exp(-\frac{U_L F\prime A_r}{\dot{m}c_p})) \quad (6)$$

The heat removal factor depends on the heat transfer fluid heat capacity, the mass flow rate and the collector efficiency factor F' which can be evaluated as

$$F' = \frac{\frac{1}{U_L}}{\frac{1}{U_L} + \frac{D_o}{h_f D_i} + (\frac{D_o}{2k} ln \frac{D_o}{D_i})} \quad (7)$$

The collector efficiency factor represents the heat exchanged between the receiver wall and the fluid, thus it depends on the thermal conductivity of the tube k and the fluid $k_f$, the heat transfer coefficient inside the receiver tube $h_f$ , and the inner and outer diameter of the receiver $D_i$ and $D_o$.

In the case of PTC, the energy balance equations are determined by conserving the energy at each surface of the surface cross section. The absorbed solar radiation by the absorber tube is conducted through the tube and eventually transferred to the heat transfer fluid by convection. The remaining heat is lost by convection and radiation inside the annular zone. The thermal energy reaching the glass tube will also be lost to the environment by convection and radiation. Figure 7 shows a schematic of the different heat fluxes interacting in the PTC heat transfer model.

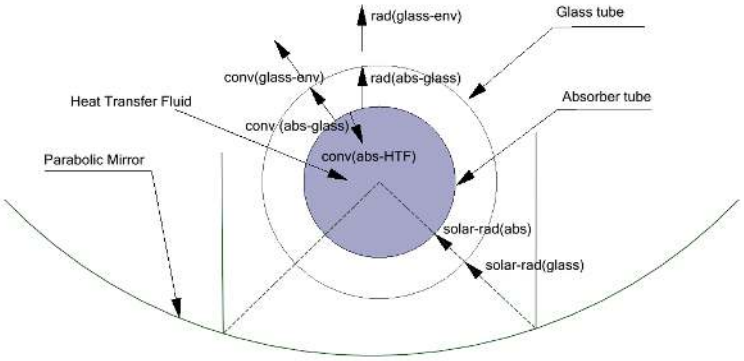


**Figure 7.** Heat fluxes interaction in the cross section of a PTC.

Various PTC energy balance models have been proposed in the literature and can be classified into two main categories: one dimensional models assuming uniform temperature distribution around the solar receiver and multi-dimensional models considering the nonuniformity of the solar flux distribution. In the

first category, the fluid domain can be solved as 0 D general model or 1D simplified model whereas in the second category the fluid domain is usually solved in 1D model. The first category is a simple and less time-consuming approach but does not provide enough information on the azimuthal variation of the temperature for the different components of the solar receiver. The latter category is more accurate and appropriate to study the effect of realistic energy flux on the optical and thermal behavior of the heat collector element (HCE) and thus more time-consuming. Moreover, it is essential to determine the temperature gradients around the HCE as well as to predict the thermal stresses and bending which should be kept under safe limits [68, 69]. In table 3 a summary of different models encountered in the literature is shown.

Table 3. Summary of different energy balance models for PTCs from the literature.

| Reference | Fluid model | Azimuthal radiation | Bracket losses | Thermophysical properties | Radiative properties |
|---|---|---|---|---|---|
| [63] | 1D | no | yes | variable | variable |
| [70] | 1D | no | no | variable | constant |
| [71] | 1D | no | yes | constant | constant |
| [72] | 0D | no | yes | constant | constant |
| [39] | 1D | yes | no | variable | constant |
| [73] | 1D | no | yes | variable | variable |
| [74] | 1D | yes | yes | variable | constant |

Discretized thermal models are the most common in thermal modeling of PTC. They are divided into one-dimensional (1D) and multidimensional models depending on the discretization strategy of the HCE. 1D models consist in discretizing the HCE along the axis direction and solving the governing energy equation as shown in Figure 8. The solar flux absorbed on the solar receiver can be either determined based on simplified optical models or considering an azimuthal heat flux radiation distribution as discussed in section 3.1.

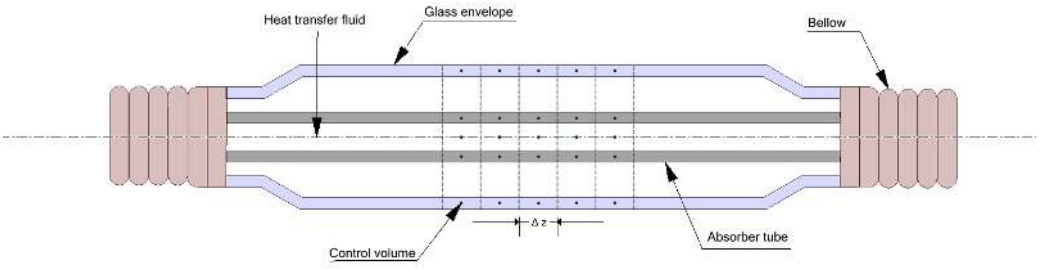


**Figure 8.** 1D model of HCE discretized on the axial direction [71].

Forristall [63] developed a comprehensive 1D model to study the effect of different design parameters and operating conditions on the PTC performance. He also compared 1 D and 2 D models under uniform solar flux condition and observed that the 1D model underestimates the heat losses for longer receivers when compared to the 2D model. Following Forristall [63], other authors [70-73, 75] used similar approaches in their 1D models, for instance, Garcia-Valladares and Velázquez [70] presented a model for a single-pass and double-pass parabolic trough collector. Padilla et al. [71] also added the effects of the thermal radiation losses between neighboring surfaces; Kalogirou [72] considered also all modes of heat transfer in each element of the collector. Yilmaz and Söylemez [73] improved the model with

comprehensive calculations of all the factors that affects the optical efficiency of the collector. Liang et at. [74] compared different 1D models under different heat transfer assumptions. They concluded that the thermal performance of PTC is predicted with good accuracy and less computational time using 1D models.

In order to take into consideration the variation of the thermal characteristics of the PTC in the azimuthal direction, a multidimensional discretization strategy needs to be implemented. In multidimensional models (2D and 3D), the HCE is discretized in both azimuthal and longitudinal directions considering the circumferential variation of the solar flux. The energy balance equation (Equation 3) is normally applied to the different components of the HCE. It is noted that the fluid side can be treated as 1D in energy balance models or 3D using a CFD model that will be discussed in section 3.2.2.

Some 2D models [76] have been developed using a uniform heat flux. In such cases, the fluid is discretized in 2D in the cross-flow direction and symmetry conditions in the axial direction are imposed. Moreover, the outer glass surface is considered isothermal. Such kind of models cannot be used for predicting the performance of the PTC due to the unrealistic boundary conditions but can be useful for studying the variations on the heat transfer coefficients inside the tube.

Other authors [77, 78] compared the uniform and non-uniform heat flux models and concluded that the uniform heat flux models can be used quickly to determine the PTC performance despite the under-prediction of the thermal losses.

Most of the multidimensional models considered the non-uniform heat flux distribution to simulate the heat transfer in the solar receiver. Hachicha et al. [39] presented a detailed thermal model based on energy balance, and coupled with an optical model to determine the temperature distribution around the solar receiver. It was noted that the circumferential temperature profile around the HCE was following the same trend of the non-uniform solar flux. Wang et al. [79] coupled a 2D model with a 3D optical model considering the nonuniformity of the energy flux density and the radiation of the side plates.

Energy balance-based models use various assumptions and correlations to estimate the different heat transfer mechanisms throughout the PTC components. Conduction and radiation heat transfer through the HCE can be treated using the basic laws and analytical formulations [80, 81]. However, appropriate correlations should be used to estimate the convection heat transfer coefficients. The heat transfer between the inner absorber tube and the HTF is due mainly to forced convection which could be either single-phase or two-phase. Most of the commercial PTC plants are using synthetic oil as HTF and therefore the majority of PTC models are based on single-phase flow approximation. A review of the correlations used to determine the heat transfer coefficient between the HTC and tube-receiver is given in [82]. The most commonly used correlation for turbulent flow in single-phase flow condition is the Gnielinski correlation [83] where Nusselt number is given as follows

$$Nu = \frac{(f_{Gni}/8)(\mathrm{Re}-1000)\,\mathrm{Pr}}{1+12.7\sqrt{(f/8)}(\mathrm{Pr}^{2/3}-1)}\left(\frac{\mathrm{Pr}}{\mathrm{Pr}_w}\right)^{0.11} \tag{8}$$

$$f_{Gni} = (1.82\log(\mathrm{Re})-1.64)^{-2} \tag{9}$$

Figure 9 shows the modeling results from different approaches (see table 3) in comparison with the experimental results for the LS2 collector. In the figure, the thermal performance obtained with the different models for both air and vacuum in the annulus is plotted. In general, the different levels of modeling yield similar results and deviations from the experimental data are within the error bars of the measurements. Out of these results, the numerical data of Garcia-Valladares et al. [70] and Liang et al. [74] deviate from the experiments, especially at low temperatures. These deviations might be due to the assumption of constant optical properties, i.e. independent on the temperature. In fact, as the model complexity increases, the accuracy in the boundary conditions and fluid model selection get more relevant to the results. Thus, appropriate conditions have to be carefully prescribed in order to obtain accurate results.

From the analysis of the foregoing, it can be concluded that 1D models can better be used for fast results although the over-prediction of the efficiency and under-prediction of heat losses increase with the length of the receiver. 2D models show a good compromise between numerical simplicity, accuracy, and fast computation. This level of modeling also allows to study influence of the variation of both optical and thermophysical properties with temperature. One-dimensional fluid models with the azimuthal distribution of the solar radiation offer the possibility of analyzing the effects on uneven heat and temperature distribution along the receiver circumference on the different parts of the HCE and the PTC performance. Moreover, these models enable the possibility, coupled with a finite-element model for solid elements, of analyzing the thermal stresses due to the heat flux variations. The use of multidimensional models for the fluid side, due to the high computational cost, are only justified if the objective is to study the impact of specific modifications in the heat collector element to improve the heat transfer such as those that will be discussed in section 5.1 (see also [84]).

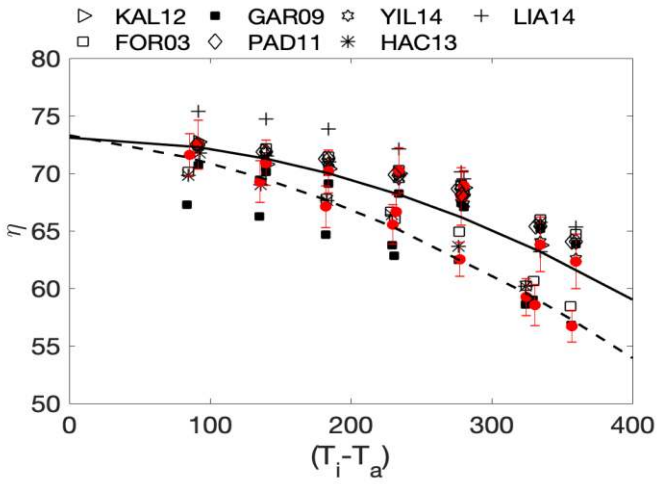


**Figure 9.** Comparison of different models for the PTC with experiments from [21] for Cermet coating. Solid line vacuum in annulus and dashed line air in annulus. KAL12 [72], GAR09 [70], FOR03 [63], PAD11 [71], YIL14 [73], HAC13 [85], LIA15 [74].

The concept of two-phase flow is mainly applied in direct steam generation (DSG) when water/steam is used as HTF. In such situation, the hydrodynamic analysis and the flow patterns are more complex and should be evaluated according to a flow pattern map. Odeh [86], based on the flow maps defined by Taitel and Dukler [87] for two-fluid flows in horizontal tubes, defined a model for evaluating the flow pattern distribution along the absorber tube of a PTC. In Figure 10, an example of the flow patterns identified by Odeh et al. [86] for a 54 mm diameter pipe is represented. In general, the flow in the absorber can be stratified, annular, dispersed, bubble or intermittent (slug or plug). The heat transfer on the fluid side depends on the flow patterns, thus different correlations for the heat transfer coefficient has to be used in order to properly predict the temperature distribution along the receiver tubes. Different DSG models have been introduced to study the thermo-hydraulic process under two-phase flow and different flow pattern maps. For instance, Serrano-Aguilera et al. [33] introduced a simple model developed for working with 3D temperature distributions in the solid parts of the PTC; Hachicha et al. [40] extended their thermo-hydraulic model for single-phase flow [39] to DSG using the flow patterns proposed by Odeh et al. [86] ; Odeh et al. [88] proposed a simplified model based on the absorber wall temperature accounting for the different fluid phases; Elsafi [89] used a different flow pattern map initially developed for refrigerants in small diameter pipes. All these models were developed, validated and tested aiming at the design and optimization of a DSG loop for a CSP plant.

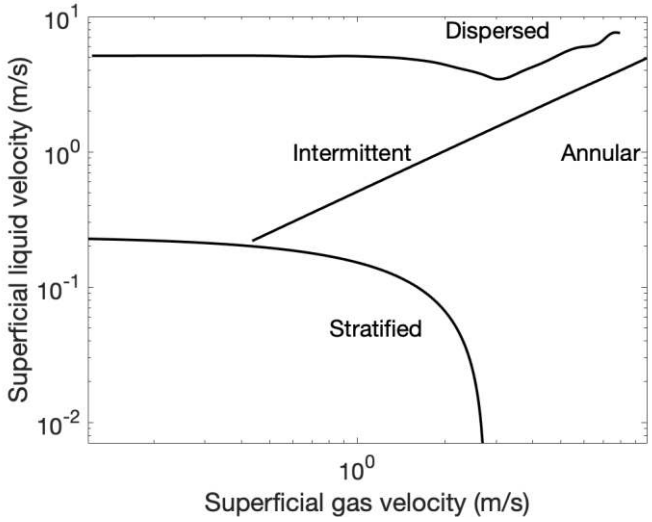


**Figure 10.** Example of flow pattern map in a HCE for DSG. Adapted from [86].

The thermal analysis of Central Receiver solar Systems can also be based on energy balances and depends on the geometry of the receiver (tubular or volumetric) as well as the heat transfer fluid (water, molten salt, air, etc.). The tubular central receiver system is the most common CRS technology and was first implemented in the early 1980s [18]. Both external and cavity type receivers can be implemented in tabular receivers (see Figure 11).

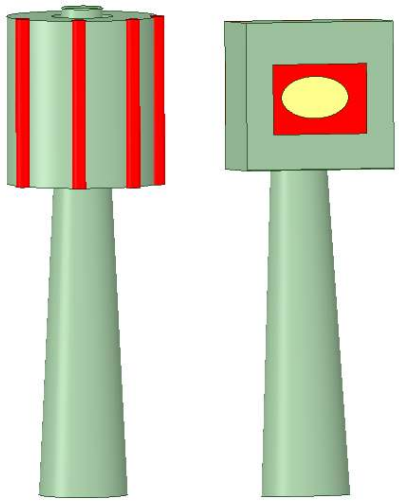

**Figure 11.** Schematic of a tubular external (left) and cavity (right) solar receiver [18].

Similar to PTC technology, CRS thermal models include the solar flux distribution on the receiver surface, convective losses and radiative losses from different elements of the solar receiver. Several models are presented in the literature (see for instance the comprehensive reviews by Behar et al. [19] and Pitot de la Beaujardiere and Reuter [90]) to study the thermal performances of central receiver systems. Most of these models focus on the estimation of thermal losses and optimizing the size of different components. The modeling of CRSs needs to consider numerous geometric and optical parameters.
Steady state energy balance models can provide the designer with an easy-to-use tool with low computational time. Under steady state conditions, the general equation of the useful energy can be expressed as follows

$$Q_u = Q_{sol,in} - Q_{loss,total} \quad (10)$$

where the total heat loss $Q_{loss,total}$ includes convective, radiative and conductive heat losses. Clausing [64] presented an analytical energy balance model to study the convective heat loss from a large cavity receiver. He concluded that thermal losses are mainly affected by the air temperature inside the cavity and the the cavity inclination, while the influence of wind on thermal losses is minimal. James and Terry [91] proposed a steady state thermal model to study the thermal performance of different geometric configurations of the cavity receiver system. They concluded that the concentrator rim has a great effect on the power profile without a significant difference in the thermal efficiency. Li et al. [92] developed a global steady state thermal model of 100 kWt molten salt cavity receiver considering a uniform incident flux. They also studied the influence of different design parameters on the thermal performance.

At the same time, the modeling of volumetric receivers is a complex process where fluid flow and heat transfer in porous structures need to be studied. Most of the published models are based on a multi-dimensional approach coupling the non-uniform flux with the CFD approach. Early models were based on a simple one-dimensional approach. Krirbus [93] proposed a one-dimensional mathematical model to study the flow and energy transfer through a volumetric absorber. He highlighted the restriction and failure mechanisms due to the high flux and flow related constraints. Bai [94] investigated the thermal performance of a silicon carbide porous media receiver based on a one-dimensional physical model. It was found that SiC has good thermal properties that lead to the increase of air outlet temperature.

A common assumption in most of the previous energy balances is a uniform heat distribution on the walls of the receiver, which is not reflecting the realistic non-uniform profiles. Therefore, to better understand the fluid flow and heat transfer under non-uniform concentrated solar flux condition, the complex coupled heat transfer should be investigated further using multi-dimensional CFD models.

### 3.2.2. CFD models

In the last decades, advances in numerical modeling have become possible due to the development of supercomputers and numerical techniques. CFD models are based on solving the Navier-Stokes and energy equations by using numerical techniques that provide detailed information on the heat transfer and fluid flow phenomena. Numerical simulations based on CFD algorithms are generally conducted through three main steps: i) pre-processing, ii) solver and iii) post-processing. The breakdown of these steps is shown in Figure 12.

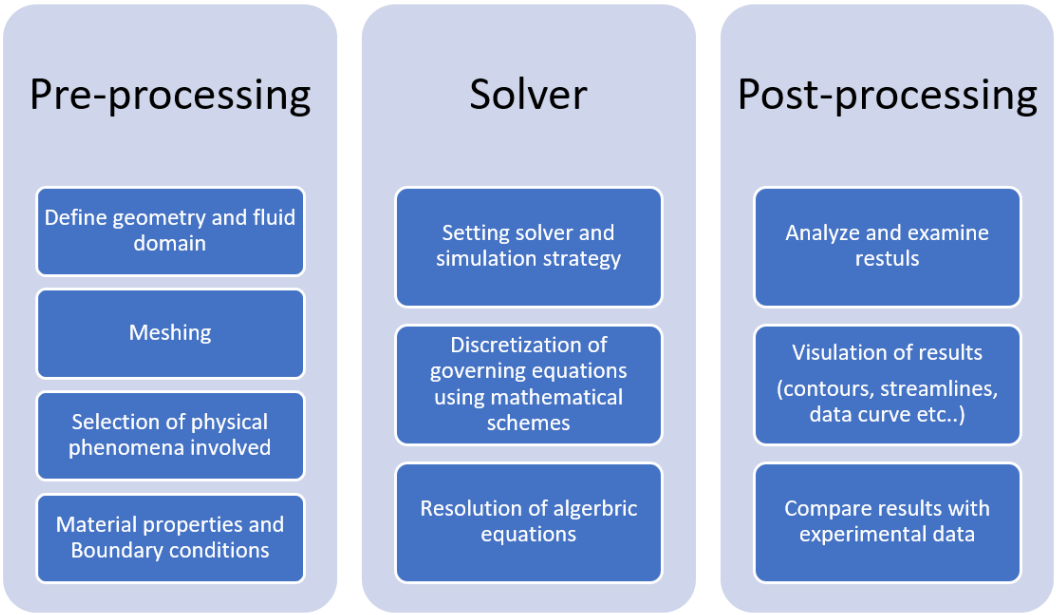

**Figure 12.** The main steps of CFD simulation process.

CFD simulations can be used to investigate new designs, analyze existing designs, and optimize the operating conditions for high-temperature solar collectors.

In PTC technology, CFD models have been used to analyze the fluid flow and heat transfer behavior of the solar receivers, as well as the wind flow around the full collector. In practice, the fluid flow inside the absorber tubes in CSP applications is under highly turbulent flow conditions. Therefore, turbulence models are usually implemented to solve the governing Navier-Stokes equations. Cheng et al. [95] used a CFD model to estimate the convection heat transfer between the HTF and the inner absorber tube, integrating the results of the optical model at the outer surface of the absorber tube. A $k$-$\varepsilon$ two-equation turbulence model with a wall function was coupled with the MCRT optical model.

He et al. [34] presented a CFD model, also based on a $k$-$\varepsilon$ two-equation turbulence model and coupled with a MCRT optical model. The model was validated with LS-2 collector tube, with an average relative error less than 2%. The authors also investigated the influence of different geometric concentration ratios and rim angles on the efficiency of the PTC. They concluded that with the increase in concentration ratios, the shadows effect become weaker, while the increase in the rim angle produces a lower value of the maximum heat flux. A similar methodology was used by Mwesigye et al. [85] with similar objectives. They showed that low rim angles produce low-temperature differences across the HCE circumference, with a trend to reduce these differences as the rim angle increases. Roldan et al. [96] used the commercial CFD package ANSYS Fluent to calculate the temperature profile and thermal stress around the absorber tube for superheated steam. They showed that the thermal gradient increases with the increase of direct solar radiation and higher steam temperature. CFD studies using non-uniform thermal boundary have also been useful for the analysis of natural and mixed convection, due to the heat flux profile [97, 98], the use of supercritical $CO_2$ as HTF [99] or the impact of the uneven flux density on the thermal stresses in PTCs [100].

All the previous CFD studies have been performed under single-phase condition. However, according to the literature, the adopted correlations used to estimate the heat transfer coefficient in the fluid lead to acceptable results [33, 82]. The main benefits of using CFD in HTF modeling is the investigation of the complex two-phase flow conditions [101, 102] and/or novel absorber designs [103-107]. On the other hand, CFD has proved to be a powerful tool to predict the wind loads around the PTC and the effect on the performance of the solar plants. Most of the aerodynamic models to study the wind loads on an isolated PTC under different configurations and wind speeds are based on Reynolds Averaged Navier-Stokes (RANS) turbulence models [108-111]. Hachicha et al., in several papers [85, 112, 113], proposed large-eddy simulations (LES) to predict the fluid flow and heat transfer around a parabolic trough solar collector for different orientations and two typical wind speeds. They concluded that the fluid flow and heat transfer behavior is a strong function of the pitch angle which may affect the stability and the overall efficiency of the collector. Figure 13 shows the resultant flow structures around the collector at different pitch angles using LES.

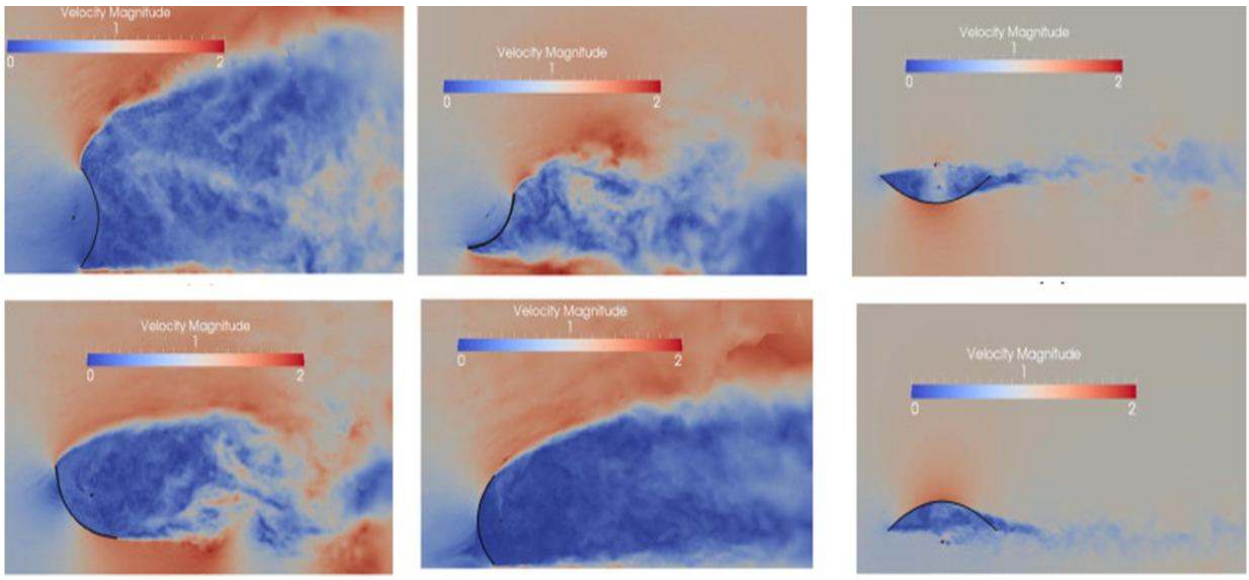


**Figure 13.** Wind flow around parabolic trough for different pitch angles using LES model [113]. (License number: 4492640292759).

Mier-Torrecilla et al. [114] used LES based on a lattice Boltzmann method (LBM) to simulate the wind loads in a model-scale, full-scale and array of PTCs. They showed that the wind loads, and the pitching moment are maximum for the exterior modules and vary remarkably along a row. Andre et al. [115] performed a LES with both lattice Boltzmann and finite element methods to estimate the wind loads on an isolated parabolic trough collector with time-varying inlet boundary condition. They observed low sensitivity of the numerical results with the modeling approaches.

CFD models have also been used by numerous authors to simulate the thermo-hydraulic behavior of CRS as well as the wind loads on heliostats. Prakash et al. [116] proposed a CFD model to study the convective losses occurring from a solar cavity receiver made up of a helical coil tube at different fluid inlet temperatures and receiver inclinations. The predicted results were compared to the experimental data with a maximum deviation of 14%. They found that the convection heat loss increases with the mean receiver temperature and decreases with the inclination.

Various CFD models [117-120] studied the thermo-hydraulic performance of tubular receivers under a non-uniform flux. The heat flux distribution around the solar receiver is usually obtained using an optical code (see section 3.1) and then integrated to the CFD model. Rodriguez-Sanchez et al. [66] compared simplified thermal models with CFD simulations for molten salt tubular receiver. They concluded that the simplified models lead to similar results to those of CFD simulations with a fast and simple way.

In volumetric receivers, the complex coupled heat transfer problem in porous structures is widely solved using CFD approach. Thermal radiation also plays an important role in heat transfer due to the high-temperature environment [121]. Some CFD models [122-124] focus mainly on the investigation of thermal performance and study of the effect of different geometric parameters and operating conditions. Other models [125-127] are more oriented towards the study of novel designs and configurations.

Besides, several CFD models have been developed to study the thermal performance of falling particles receivers which show high potential in achieving high temperatures up to 1000°C [128]. Multiple configurations and designs were investigated using CFD models and can be classified according to the way of heating: directly [129-131] or indirectly [132, 133].

In addition, aerodynamic modeling in central receiver systems is essential to simulate the heat losses from the solar tower as well as the stability of the heliostat and the optical performance under windy conditions. As the temperature of the solar receiver gets higher than the ambient temperature, a significant amount of energy is lost to the surrounding by conduction, convection and radiation. Although in these

receivers conduction losses can be considered rather small, heat losses by radiation and convection are complex and need to be studied.
A review on the research studies on thermal losses from cavity receiver is presented in [134]. In order to consider the effect of wind, CFD models have been developed to study and predict the heat losses by natural [135-137], forced [116, 138] and mixed convection[139, 140]. Roldan et al. [141] proposed a CFD model to investigate the thermal efficiency of an open volumetric receiver under wind and return-air conditions. They showed that thermal performance is more affected with wind at higher magnitude and direct incidence direction.
At the same time, the aerodynamic modeling of heliostat plays an important role in the prediction of the wind effects on the stability and optical performance. Various CFD models have been developed to study the wind effect on heliostat and photovoltaic trackers as they are similar cases. Most of the published models are based on RANS models [142, 143], while other authors[144-146] recommended the use of more suitable turbulence models such as LES and detached eddy simulations (DES) to well capture the fluid structures around the heliostat.

### 3.3. Dynamic models

In all the previous modeling approaches, steady-state conditions are assumed for the sake of simplicity. However, in practice CSCs are under transient conditions as the weather conditions are changing with time and the effect of startup and shutdown does not allow the long operation under steady conditions. Dynamic models can be categorized into two main areas depending on the considered system: i) transient flow models dealing with the transient behavior of the HTF and ii) plant performance models focusing in the transient characteristics of the solar plant.
In PTC technology, various dynamic models have been published [147, 148] to predict the thermal and overall performances under transient conditions. Transient flow models are proposed to study the effect of unsteady parameters for both single-phase and two-phase flow. Numerous studies proposed are based on lumped capacitance models mainly one dimensional [149-151] and few multidimensional models [152].
Other scholars [153, 154] presented transient models to simulate the complex transient behavior of DSG in PTC and predict the thermal instabilities in DSG loops. Moreover, the transient simulation of the dynamic performance of the plant has been the subject of other works using different software tools such as; TRNSYS [155], Modelica [156], and SAM [157]. Such models are very useful to evaluate the dynamic performance, plant operation strategies and assess new ideas and configuration in the design phase.
Similarly, dynamic models for CRS technologies can also be classified into two main categories: lumped capacitance models and plant performance models. The lumped capacitance models [158-161] are devoted to predicting the dynamic characteristics and thermal losses without considering the simulation of the whole plant. The majority of dynamic models in CRS focused on the modular modeling of the whole solar plant to determine the output power. Various simulations tools have been used to simulate the whole CRS plant such as ; TRNSYS[162] , SOLERGY[163], MODELICA [164] and STAR-90[158]. Most of these models were coupled with optical codes to determine the flux maps on the receiver.

## 4. Attributes and applicability of the modeling approaches

Numerical modeling is an important tool to design, simulate and optimize different components of CSCs. This tool is not only used to study and analyze the performance of existing solar plants but can be also explored to design and optimize new CSP projects. However, experimental works remain essential to validate and test the various practical aspects of proposed models.
The aforementioned modeling approaches have been analyzed and compared in order to assess their predictive capabilities and suitable application for each approach. In this section, the main merits and demerits of these modeling approaches are discussed, highlighting the applicability and effectiveness for the current and future CSC applications.

**Optical models:** It is obvious that optical modeling is crucial in CSC where the flux is not uniform due to the optics of the different concentrator components. The use of accurate and efficient optical models that can deal with the non-uniform flux distribution, but also take into account optics and tracking errors is of major importance. Such a tool is not only required for the detailed analysis of the optical performance but also in system design and optimization. Moreover, the output of the optical modeling is essential to understand the temperature distribution and therefore the thermal performance of CSCs. This can be achieved by integrating both optical and thermal models in a comprehensive modeling strategy. For this purpose, it is a common practice to assume the optical properties independent to temperature and consider the optical modeling as a pre-processing to the general performance model.

In general, the analytical/simplified models give accurate results with less computational time, although the mathematical complexity of such models makes them not very practical in certain cases. These models includes several optical parameters as a function of the concentrator configuration in order to determine the optical performance of CSC systems. However, this modeling approach is mainly used for simple geometry and may have some errors due to incomplete description of reflective surfaces and sun shape properties [26].

Ray tracing techniques and the optical codes are more preferred in the optical modeling with more flexibility to be integrated into a general thermal model. These models are more appropriate to accurately study the three-dimensional optical effects when various optical errors, due to reflector curvature, mirror qualities and tracking errors, are present [53, 165]. Besides, ray tracing models are more feasible and reliable to study and optimize new CSC designs with non-ideal optics [25]. This approach is commonly used in commercial and scientific works as well as various software tools such as SolTrace, Tonatiuh, DELSOL, Raytrace3D. However, the computational time required by these computer-based tools is quite significant and depends on the development of computer technology.

**Thermo-Fluid models:** The main objective of thermo-fluid models is to study the steady thermal performance of CSCs under different operating conditions and the possible improvements that can be made. Energy balance models are simpler and faster models since they deal with solving the energy equations only. In such cases, empirical correlations are used to estimate the heat transfer on the HCE. Depending on the way of discretizing the HCE, energy balance models are classified into one dimensional and discretized models. One dimensional models are limited as they cannot consider the non-uniformity of the heat flux. Despite this fact, these models could be employed to quickly evaluate the integral heat transfer performance of CSCs with a good proximity to experimental results [78, 166].

On the other hand, discretized models are more time consuming but more suitable to simulate the non-uniform temperature distribution. These models are more recommended for evaluation of the thermo-hydraulic behavior for long absorber tubes especially when the pressure drop and the non-uniform effects are prominent. Nevertheless, the use of discretized models is also beneficial in case of two-phase flow due to the interaction between the non-uniform heat flux and two phase flow that lead to higher complexity level.

In complex geometries and designs purposes, CFD is more appropriate to model the coupled fluid flow and heat transfer present in CSC. Taking the advantages of the advances in computer technology, these models are well suited to simulate, analyze and optimize new designs as well as to assess the practical limits.

Both internal and external flow around the CSC can be predicted using CFD models with adequate turbulence models for high Reynolds numbers. RANS models are more suited in CSC modeling for industrial applications, as they need less computational time than advanced models (LES, DES, DNS). However, in order to capture the detailed flow structure and to understand the main transfer mechanisms present, advanced models are required.

CFD models are usually time-consuming models especially in complex geometries. In PTC applications, CFD modeling is very useful to study the different techniques of performance enhancement but also to examine the thermal stress around the HCE.

On the other hand, CFD simulation is more challenging in the case of CRS where different length scales may be present. Despite of this, CFD modeling has a potential capability in modeling porous structures and free-falling receivers where the thermo-hydraulic behavior is more complex.
In general, energy balance models can be more practical, less time consuming and suitable for an easy decision-making on the initial design, whereas CFD models are interesting for design and optimization of CSCs.

**Dynamic models:** This approach is used to assess the thermal performance of CSCs under transient conditions, taking into consideration the various fluctuations from the startup to the shutdown. It is also of great use to develop control strategies and optimize the thermodynamic cycle as well as the thermal energy system. These models can be divided in two categories depending on the component or full system perspective: lumped capacitance and plant performance models.
The simplified lumped capacitance models are mainly used to determine the dynamic behavior of the HTF and the resultant heat transfers of the CSC. Such models are more appropriate to predict the dynamic variation of CSC characteristics and controllability strategies under different flow conditions. Such models become more relevant in case of two-phase flow, which is highly affected by the dynamic conditions throughout the different stages of the solar field. Moreover, they are less time consuming and provide a reasonable prediction of the transient behavior.
However, they are not capable of assessing the interaction of the solar receiver with the other components and evaluating the dynamic performance of the whole solar plant. For such needs, it is recommended to use plant performance models, which can be used in the operational and design phase to assess the use of new designs. These models are more appropriate for the study and evaluation of the plant performance from a process dynamics point of view. For that reason, they could be easily integrated in a comprehensive life-cycle analysis to assess the techno-economic feasibility of CSP plants. Most of these models used software tools (TRNSYS, Modelica, SOLERGY) that integrate the various components of the solar plants, coupled with optical codes. Using these platforms, it is possible to evaluate the final energy output of the whole solar plant for performance prediction and optimization. One of the important features of these models is the flexibility to integrate the TES system as well as hybridization of the solar plant with other energy sources.
In order to provide a guideline for the modeling of high temperature solar collectors, the above model approaches have been compared in terms of different selection criteria. Table 4 shows the main characteristics and level of difficulty of the studied models for evaluating the performance of existing and novel designs of CSC systems.

Table 4. Comparison of the studied models based on selection criteria and level of difficulty.

| **Characteristics/ Criteria** | **Optical Models** | | **Thermo-Fluid Models** | | **Dynamic Models** | |
|---|---|---|---|---|---|---|
| | Analytical/ simplified | Ray tracing | Energy balance | CFD | Lumped capacitance | Plant performance |
| **Mathematical model** | Average | Complex | Simple | Complex | Simple | Complex |
| **Accuracy** | Average to High | High | Average to High | High | Average to High | Average to High |
| **Computational time** | Low | High | Low | High | Low | High |
| **Modularity** | Difficult | Yes | Yes | Difficult | Difficult | Yes |
| **Considering non-uniform flux** | Difficult | Yes | Yes | Difficult | Difficult | Yes |

| | | | | | | |
|---|---|---|---|---|---|---|
| **Adaptability for new designs** | Difficult | Yes | Difficult | Yes | Yes | Difficult |
| **Adaptability for plant simulation** | Difficult | Yes | Yes | Difficult | Difficult | Yes |

## 5. New trends in performance enhancement

Based on the aforementioned modeling approaches, new techniques of performance enhancement have been studied in the literature [10, 18, 167] to operate the CSCs at a higher temperature and higher efficiency. These techniques can range from modifying the solar collector design to changing the heat transfer fluid properties by using nanofluids[167]. In such situations the heat transfer enhancement can be evaluated based on the well-known Nusselt number *Nu*. Moreover, the friction factor *f* needs to be determined in case of a pressure drop penalty which leads to an increase of the pumping power. In both cases, the numerical results supported the hypothesis of performance enhancement with respect to a reference case, which can be evaluated using the performance evaluation criterion (PEC) [168].

$$PEC = \frac{\left(\frac{Nu}{Nu_0}\right)}{\left(\frac{f}{f_0}\right)^{1/3}} \quad (11)$$

Where $Nu_0$ and $f_0$ represent the Nusselt number and friction factor of the reference case.

Alternative techniques also aim to reduce the cost of investment and operation as well as to improve the environmental impacts of CSCs. However, the technical feasibility and experimental validation are needed to move these techniques towards the full commercial scale.

### 5.1. New designs

Many authors proposed novel designs [10] to improve the optical and thermal performance of PTC technology. Significant efforts were made to modify the shape of heat collector elements using internal fins, dimples and other geometrical changes. Other works [169, 170] have been focused on introducing flow inserts and turbulators which enhance the turbulence intensity and promote the increase of the effective heat transfer area. However, many of these techniques lead to an increase in pressure loss, and therefore to higher required pumping power and more complex hydraulic installation.

Most of these studies are based on CFD modeling to have a good insight into the fluid flow and heat transfer, and understand the thermo-hydraulic performance of the enhanced design. Other authors used energy balance models and available empirical correlations for a quick assessment. Table 5 summarizes the most relevant numerical studies using new techniques of enhancement for PTC technology.

Additionally, new designs of central receiver system have been proposed based on numerical models to replace the conventional tubular receivers. Various enhancement techniques proposed for PTC technology have also been studied for tubular receivers where a higher degree of turbulence is induced by enlarging the effective heat transfer area and generating secondary/swirl flow. In addition, emerging particle, gas and liquid based technologies are investigated, and new modifications have been evaluated based on numerical modeling. Selected numerical models of innovative designs are given in Table 6. The outcome of these studies is of great interest for the development of CSC technology, but more experimental works with an emphasis on the durability and large-scale implementation are still needed.

Table 5. Summary of the numerical models adapted for new PTC designs.

| Reference | Novel design | | Increase | | | | Models | | Tools |
|---|---|---|---|---|---|---|---|---|---|
| | Modification | Working fluid | Heat transfer | Friction factor | PEC | $\eta_{th}$ | Approaches (optical/thermo-fluid) | Properties | |
| **[171]** | Wall detached twisted tape inserts | Syltherm 800 | 1.05–2.69 | 1.6-14.5 | - | 10 % | MCRT/CFD | Turbulence model: Realizable k-ε | SolTrace/ANSYS |
| **[172]** | Twisted tape | Water | 3% | 26 | - | 9% | Simplified/1D energy balance | Empirical correlations for Nu | In house code |
| **[173]** | Helical screw-tape inserts | Dowther m A | 6 | 23 | - | - | MCRT/CFD | Turbulence model: SST k–ω | Matlab/ANSYS |
| **[107]** | Louvered twisted-tape inserts | Behran oil | 37%-150% | 72%-210% | - | - | Simplified/CFD | Turbulence model: RNG k-ε | ANSYS |
| **[174]** | Twisted tapes with six twist ratios | Molten salt | 250% | 120% | - | - | Simplified/CFD | Turbulence model: RNG k-ε | ANSYS |
| **[105]** | Perforated plate | Syltherm 800 | 8-133.5% | 1.4-95 | - | 8% | MCRT/CFD | Turbulence model: Realizable k-ε | SolTrace/ANSYS |
| **[175]** | Wavy-tape inserts | Syltherm 800 | 261%-310% | 382-405% | 2.11 | - | MCRT/CFD | Turbulence model: Realizable k-ε | ANSYS |
| **[176]** | Unilateral longitudinal vortex generators | Syltherm 800 | 50% | 88% | 1.18 | - | MCRT/CFD | Turbulence model: Realizable k-ε | ANSYS |
| **[177]** | Dimpled receiver | Thermino l VP-1 | 1-21% | 1-34% | - | - | MCRT/CFD | Turbulence model: Realizable | ANSYS |

| | | | | | | | | | |
|---|---|---|---|---|---|---|---|---|---|
| | | | | | | | | k-ε | |
| **[103]** | Metal foam | Water/steam | 10-12 times | 400-700 times | 1.5 | - | MCRT/CFD | Turbulence model: Standard k-ε | ANSYS |
| **[178]** | Asymmetric outward convex corrugated tube | D 12 oil | 59% | 30% | 1.48 | - | MCRT/CFD | Turbulence model: Realizable k-ε | ANSYS |
| **[179]** | Porous rings | Syltherm 800 | 37% | - | - | - | Simplified/CFD | Turbulence model: RNG k-ε | ANSYS |
| **[180]** | Converging-diverging tube | Therminol VP-1 | 37% | 106% | - | 4.5 % | Simplified/CFD | Empirical correlations for Nu | Solidworks |
| **[181]** | Internal longitudinal fins | Syltherm 800 | 65% | 50% | - | 0.82 % | Simplified/CFD | Turbulence model: Standard k-ε | Solidworks |
| **[104]** | Internal helically finned tube | Syltherm 800 | - | 50% | - | 3% | Simplified/CFD | Turbulence model: RNG k-ε | ANSYS |
| **[182]** | Sinusoidal absorber tube | Syltherm 800 | 45-63% | 40% | 1.35 | - | MCRT/CFD | Turbulence model: SST k-ω | Tonatiuh/ANSYS |
| **[183]** | Wire coil | Water | 2.28 | - | - | - | CFD | Turbulence model: Standard k-ε | ANSYS |

Table 6. Summary of the numerical models adapted for new CRS designs.

| Reference | Novel design | | Models | | Tools | Remarks |
|---|---|---|---|---|---|---|
| | Modification | Working fluid/medium | Approaches (optical/ thermo-fluid) | Properties | | |
| **[184]** | helically coil/wire, twisted tape insert, and dimpling for the tubular gas receiver | Air , $CO_2$, He | Simplified/Energy balance | 3D model | In house code | An optimum PEC of 2.1 could be achieved with the dimpled tube. |
| **[185]** | Use heat pipe for cavity receiver | Molten salt | Simplified/CFD | 3D laminar flow | ANSYS | Increase of 1% in receiver efficiency respect to the molten salt receiver. |
| **[119]** | hexagonal pyramid-shaped elements | Molten salt | Simplified/CFD | Turbulence model: Standard k-ε | ANSYS | Thermal efficiency of the new receiver reached 91.2% at an incident power of $1MW/m^2$. |
| **[186]** | Jet impingement | Molten salt | MCRT/CFD | Turbulence model: SST k-ω and LES | SolTrace/Ansys | Convection heat transfer increases as the flow accelerate away from the stagnation point. |
| **[187]** | Recirculating flow solid particle solar receiver | Air and micron size Bauxite $Al_2O_3$ particles | Simplified/CFD | Discrete particle model, Do radiation model and RNG k-ε turbulence | ANSYS | An increase of 30% in thermal efficiency is observed compared to vortex flow receiver. |
| **[131]** | Particulates flow through a porous medium | Air with fracking sand | Simplified/CFD | Eulerian-Eulerian tow-fluid model | ANSYS | Using ordinary particulate a temperature of 1000 °C can be achieved. |
| **[188]** | Several panels of bayonet tubes | Molten salt | Simplified/Energy balance | 2D model Empirical correlations | In house code | The maximum film temperature and the maximum wall temperature decreased by 84 °C and 100°C, respectively. Thermal efficiency increases by 2%. |
| **[189]** | Three different geometry shapes | Air | MCRT/CFD | Turbulence model: | ANSYS | The conical achieved the highest thermal efficiency of about 77.05%. |

| | | | | | | |
|---|---|---|---|---|---|---|
| | of receiver: cylindrical, conical and spherical | | | Standard k-ε | | |
| **[190]** | Annular reticulate porous ceramic bounded by two concentric cylinders | Air | MCRT/Energy balance | 2D FVM Rosseland approximation | MATLAB | The novel receiver achieved an outlet air temperature of 1000° C and thermal efficiency of 78% at concentration ratio of 3000 suns. |

### 5.2 Use of nanofluids in CSCs

Thermophysical properties of the HTF are enhanced using suspended nanoparticles. The addition of nanoparticles results in increased heat transfer coefficient, improved thermal conductivity, as well as reduced thermal boundary layer thickness, and therefore enhancing the thermal efficiency of CSCs [191]. Solid nanoparticles ( 1-100nm) suspended in conventional fluids is an alternative method for increasing the heat transfer rate due to their higher thermal conductivities [192]. Drawbacks such as clogging, sedimentation, and high-pressure drop are prevented due to the small size of the nanoparticles [193]. This new class of heat transfer fluid was first introduced [194, 195] nearly two decades ago, and since then much research has been carried out in this field to either study or enhance its properties. Nanofluids are mainly characterized into two groups of metallic (Al, Fe, Ag, Cu) and non-metallic ($Al_2O_3$, $TiO_2$, $Fe_2O_3$, CNTs, graphene, and hybrid/composite) nanofluids [196]. Addition of small weight fractions of the nanoparticles to the conventional fluids results in enhanced thermophysical properties.

Numerous studies have been reported using nanofluids as HTF for PTC both numerically and experimentally [84]. The experimental results reported by the authors showed that the stability and thermal conductivity of the nanofluids depend strongly on the volume fraction, pH and duration of sonication time [197]. Some researchers used surfactants as a stabilizing agent to stabilize the nanofluids for CSP collectors [198]. However, it has already been reported widely in the literature that using surfactant can stabilize the nanofluids at a lower temperature, but at a higher temperature, they melt due to their lower melting temperature, and therefore resulting in sedimentation of the nanofluid [192].

In addition, many scholars [199, 200] developed various numerical models to investigate the use of different combinations of nanoparticles and base fluids for possible performance enhancement. Recent numerical studies reported using nanofluids in PTC technology are presented in Table 7. It is clear from these studies that energetic and exergetic efficiencies using both the mono and hybrid nanofluids are favorable and would result in making PTCs a more competitive and sustainable energy technology [201]. However, using high volume fractions of nanoparticles might result in poor thermal characteristics due to the reduced zeta potential value of the nanofluids, that results in sedimentation of the nanoparticles. Most of the studies reported for these systems have not taken into

consideration the stability of nanofluids for a long period, which is crucial for using nanofluids as HTF. More studies using hybrid nanofluids are recommended to be further investigated both numerically and experimentally. The detailed exergoeconomic analysis is also recommended, to show the usefulness of nanofluids in these systems at all range of temperatures. New trends in using nanofluid combined with the passive method and in porous absorber media are considered as promising future studies for heat transfer enhancement.

Table 7. Summary of the numerical models adapted for PTC with nanofluids.

| **Reference** | **Nanofluid** | | **Increase** | | | | **Models** | | **Tools** |
|---|---|---|---|---|---|---|---|---|---|
| | Base fluid | Nanoparticle | Heat Transfer | Friction factor | PEC | $\eta_{th}$ | Approaches | Properties | |
| **[202]** | Thermal oil | MWCNT | 15% | - | - | 0.5% | Simplified/energy balance | 2 D and uniform flux | Matlab |
| **[203]** | Synthetic oil | $Al_2O_3$ | 14% | - | - | - | MCRT/CFD | Turbulence model: Standard k-ε | Ansys |
| **[204]** | Water | CuO, $Al_2O_3$ | 28%-35% | 50% | - | - | Simplified/CFD | Turbulence model: RNG k-ε | Gambit/ANSYS |
| **[205]** | Therminol 66 | $Al_2O_3$ | 56% | 6 times | 1.25 | - | Simplified/CFD | Turbulence model: RNG k-ε | ANSYS |
| **[206]** | Therminol VP-1 | Cu | 32% | - | - | 12.5 % | MCRT/CFD | Turbulence model: Realizable k-ε | SolTrace/ANSYS |
| **[207]** | Therminol VP-1 | Ag, Cu, $Al_2O_3$ | 7.9%, 6.4%, 3.9% | - | - | 13.9\| % | MCRT/CFD | Turbulence model: Standard k-ε | ANSYS |
| **[208]** | Therminol VP-1 | SWCNT | 234% | - | - | 4.4% | MCRT/CFD | Turbulence model: Realizable k-ε | SolTrace/Ansys |
| **[209]** | Syltherm 800 | $Al_2O_3$ | - | - | - | 1.2% | MCRT/CFD | Turbulence model: k-ω | SolTrace/Ansys |
| **[210]** | Syltherm 800 | $Al_2O_3$ | - | - | - | 10% | MCRT/CFD | Curve fitting used for the flux distribution | ANSYS |

| | | | | | | | | | |
|---|---|---|---|---|---|---|---|---|---|
| **[180]** | Thermal oil | $Al_2O_3$ | 9% | 5% | - | 4.25 % | Simplified/CFD | Turbulence model: Standard k-ε | Solidworks |
| **[169]** | Syltherm 800, Molten salt | CuO | 40% | 40% | - | 1.54 % | Simplified/CFD | Turbulence model: Standard k-ε | Solidworks |
| **[211]** | Water/ 60EG:40W | Ag-MgO, $Al_2O_3$-Cu, GO-$Co_3O_4$ | 14% | 23% | - | 5% | Simplified/CFD | Laminar flow subjected to constant heat flux is considered | Fortran |
| **[212]** | Water | CuO, $Al_2O_3$, SiC | 29%, 19%, 16% | - | - | 13.91 % | Simplified/Energy Balance model | Solar flux is uniform Empirical correlation are used | Matlab |
| **[213]** | Synthetic oil | CuO, $Al_2O_3$, $TiO_2$ | 32-83% | - | - | 1.64 % | Simplified/dynamic | 1D unsteady model | Matlab |
| **[214]** | Synthetic oil | $Al_2O_3$ | - | - | - | 14.3 % | MCRT/CFD | Turbulence model: RNG k-ε | SolTrace/ In house code |
| **[201]** | Syltherm 800 | $Al_2O_3$, $TiO_2$, $Al_2O_3$-$TiO_2$ | 178% | | | 1.8% | Simplified/ Energy balance model | Empirical correlations are used for Nu | EES |

There is a gap in the literature in the area of using nanofluids as HTF numerically and experimentally in solar towers, this limitation could be due to the large amount of nanoparticles that would be required for such systems as well as the cost of the experimental setup for validation purposes. Nevertheless, nanofluids have been investigated in volumetric receivers for high-temperature applications. Some authors proposed the use of nanofluids for direct steam generation at high solar concentrations. Jin et al. [215] performed experimental and numerical studies on the use of gold nanoparticles in a cylindrical receiver at a concentration ratio of 220 suns. A photothermal efficiency of 80.3% was obtained for 12.75 ppm of gold nanoparticles [215]. There is still a lack of strict experimental proof and well-established mechanism analysis for a solar steam generation [216, 217]. Other authors introduced the use of nanofluid in direct absorption volumetric receivers which are beamed with concentrated sunlight and directly absorbed with the nanofluid [218] or molten salt with nanoparticles [219]. Using nanofluids in these systems may reduce the temperature difference between the fluid and the receiver surface, due to the higher surface area of the nanoparticles [220, 221] and higher thermal conductivity which results in improved heat transfer mechanism [221, 222].
Some researchers suggested the use of micro/nano particles in volumetric absorption solar collectors [220, 223]. Energy balance, CFD and dynamic models are used to simulate the combined radiative and convective heat transfer phenomena inside particle-based receivers [224]. Despite the multiple features of such models, the optimal design of volumetric solar flow receiver is not fully clear [225]. Selected numerical studies of nanofluid-based volumetric receivers are summarized in table 8.

Table 8. Literature review of numerical studies of nanofluid-based volumetric receivers.

| Reference | Nanoparticles /Basefluid | Model approaches and properties | Tools | Remarks |
|---|---|---|---|---|
| **[226]** | Mono disperse cobalt oxide in nitrate salt | Energy balance model/Discrete Ordinate Method for spectral radiation | In house code | The increase of volume, particle diameter or film width lead to an increase of the thermal efficiency. |
| **[227]** | Carbon particles (0.5 μm) in air | 3D energy balance model including radiative transfer equation | In house code | The results are fairly independent to the particle size and large temperature gradients observed in case of oxidation. |
| **[228]** | Aluminum, copper, graphite and silver nanoparticles in Therminol VP-1 | Energy balance equation /1D radiation transport equation | In house code | The efficiency is improved by 5 to 10% using nanofluid.<br>A yearly gain of $3.5 million could be added for a 100$MW_e$ nanofluid solar tower. |
| **[229]** | Micron size Bauxite metallic particles in air | CFD model / discrete model and RNG k-ε model<br>Discrete ordinate method is used for radiation modeling | ANSYS | The thermal efficiency is enhanced by 2 times with recirculating the air and particle mixture. |
| **[230]** | Graphene dispersed in $[HMIM]BF_4$ | 1D dynamic model (lumped capacitance) with radiative transfer equation | MATLAB | The thermal efficiency of increases with solar concentration and receiver height but decreases with graphene concentration.<br>Thermal efficiency of |

| | | | | |
|---|---|---|---|---|
| | | | | 70% is obtained for 0.0005% of graphene under 20 solar concentration and 600K. |
| **[231]** | Carbon-coated nanoparticles (28 nm) in Therminol VP-1 | 1D dynamic model (lumped capacitance) including radiative transfer equation<br>Finite difference scheme and Runge-Kutta method are used for the transient solution | In house code | System efficiency exceeds 35% for solar concentration above 100 and nanofluid height above 5 cm. The design can be well suited for down beam CSP systems. |
| **[217]** | Graphitized carbon black, carbon black, and graphene suspended ( 0.5 wt.%) in water | 1D dynamic model (lumped capacitance) including radiative transfer equation | COMSOL | A maximum vapor generation efficiency of 69% is reported at 10 suns using nanofluid |

Based on the literature review, there is a need to increase the efficiency of direct solar vapor generation process at higher solar concentration for the technology to be more applicable and cost effective. There is also a need to further work on numerical modeling for these systems and more parametric studies should be carried out to fully understand the coupled radiative and heat transfer mechanisms. Some of the future recommendations in this direction are as follows:

- More economical studies on the use of nanofluids in CSCs are required.
- There is a need for developing new numerical models especially for CRS technology
- Studies are needed to show nanofluids effect in the CSCs regarding corrosion and erosion when used as HTF. Careful design of the systems are needed due to the toxicity of nanofluids.

## 6. Conclusions

A review of the various modeling approaches adopted to simulate the most dominant CSP technologies, i.e. parabolic trough and central receiver systems is presented in this paper. These modeling approaches provide a powerful tool to simulate and predict the different optical, thermal and dynamic performances of CSCs as well as to assess novel designs and possible improvements. The modeling of such collectors offers a unique opportunity to study existing installations and new improvements under realistic conditions with a low-cost strategy compared to experimentation. Nevertheless, experimental studies remain essential to test the validity and capability of these modeling approaches.
From the reviewed studies, it is found that the modeling of CSCs can be classified into three main categories: optical, thermo-fluid and dynamic. The first category refers mainly to the estimation of the realistic non-uniform flux around the high-temperature receivers. Ray tracing models are shown to be more appropriate to determine the optical characteristics and to optimize the optical characteristics of new designs where the analytical solution cannot be easily applied. The second category includes different modeling strategies which aims to determine the thermo-hydraulic performance of CSCs under different operating conditions. Depending on the required level of accuracy energy balance and CFD models can be selected in this category. The energy balance models are simple and can be used as a quick evaluation tool for CSC technology with reasonable accuracy. However, CFD models are more convenient to study new/complex designs and elaborate detailed flow analysis at the expense of a higher computational cost. Both internal and external flows can be studied using CFD tools where wind conditions can alter the overall performance of these collectors. The last category involves the assessment of the CSCs under the transient condition and its implication for the whole power plant. It is concluded that lumped capacitance models are more suitable to study the

dynamic behavior of the solar receiver, whereas the plant performance models can give an insight on the evolution of the whole solar plant under variable operating conditions.

In addition to that, numerical modeling is also a key element in studying new trends of CSP technologies including innovative designs and use of nanofluids. These techniques have shown promising results in enhancing the thermal performance of the CSCs which could have a major impact in reducing the levelized cost of electricity in CSP plants. However, there is still a need to conduct further research to validate these techniques at large scale and investigate the life cycle analysis. The use of nanofluids in PTC technology has been widely discussed in the literature but some drawbacks such as the long-term stability and corrosion need to be further studied. Moreover, environmental and exergoeconomic analysis could also help to evaluate the usefulness of nanofluids at higher operating temperatures. Unlike PTC, the numerical studies on the use of nanofluid in CRS are mainly focused on volumetric receivers. Steam generation and direct absorption solar collectors at high concentrations are hot topics for the potential use of nanofluids in CRS technology. Nevertheless, more numerical models and experimental validations are needed to justify the applicability and cost-effectiveness at large scale.

**Acknowledgements**

The first author would like to thank University of Sharjah, Project #1702040679-P, and Sharjah Electricity and Water Authority (SEWA), Project #1702040683-P for their support.

**List of References**

1. Mekhilef, S., R. Saidur, and A. Safari, *A review on solar energy use in industries.* Renewable and Sustainable Energy Reviews, 2011. **15**(4): p. 1777-1790.
2. Grätzel, M., *Solar Energy Conversion by Dye-Sensitized Photovoltaic Cells.* Inorganic Chemistry, 2005. **44**(20): p. 6841-6851.
3. Stein, W.H. and R. Buck, *Advanced power cycles for concentrated solar power.* Solar Energy, 2017. **152**: p. 91-105.
4. Timilsina, G.R., L. Kurdgelashvili, and P.A. Narbel, *Solar energy: Markets, economics and policies.* Renewable and sustainable energy reviews, 2012. **16**(1): p. 449-465.
5. Zhang, H.L., et al., *Concentrated solar power plants: Review and design methodology.* Renewable and Sustainable Energy Reviews, 2013. **22**: p. 466-481.
6. Izquierdo, S., et al., *Analysis of CSP plants for the definition of energy policies: The influence on electricity cost of solar multiples, capacity factors and energy storage.* Energy Policy, 2010. **38**(10): p. 6215-6221.
7. Lilliestam, J. and R. Pitz-Paal, *Concentrating solar power for less than USD 0.07 per kWh: finally the breakthrough?* Renewable Energy Focus, 2018. **26**: p. 17-21.
8. Blanco, M. and L.R. Santigosa, *Advances in Concentrating solar thermal research and technology*2016: Woodhead Publishing.
9. Islam, M.T., et al., *A comprehensive review of state-of-the-art concentrating solar power (CSP) technologies: Current status and research trends.* Renewable and Sustainable Energy Reviews, 2018. **91**: p. 987-1018.
10. Bellos, E. and C. Tzivanidis, *Alternative designs of parabolic trough solar collectors.* Progress in Energy and Combustion Science, 2019. **71**: p. 81-117.
11. Liu, M., et al., *Review on concentrating solar power plants and new developments in high temperature thermal energy storage technologies.* Renewable and Sustainable Energy Reviews, 2016. **53**: p. 1411-1432.
12. Vignarooban, K., et al., *Heat transfer fluids for concentrating solar power systems–a review.* Applied Energy, 2015. **146**: p. 383-396.
13. Yılmaz, İ.H. and A. Mwesigye, *Modeling, simulation and performance analysis of parabolic trough solar collectors: A comprehensive review.* Applied Energy, 2018. **225**: p. 135-174.
14. Müller-Steinhagen, H. and F. Trieb, *Concentrating solar power.* A review of the technology. Ingenia Inform QR Acad Eng, 2004. **18**: p. 43-50.
15. Fuqiang, W., et al., *Progress in concentrated solar power technology with parabolic trough collector system: A comprehensive review.* Renewable and sustainable energy reviews, 2017. **79**: p. 1314-1328.

16. Abdulhamed, A.J., et al., *Review of solar parabolic-trough collector geometrical and thermal analyses, performance, and applications.* Renewable and Sustainable Energy Reviews, 2018. **91**: p. 822-831.
17. Fernández-García, A., et al., *Parabolic-trough solar collectors and their applications.* Renewable and Sustainable Energy Reviews, 2010. **14**(7): p. 1695-1721.
18. Ho, C.K. and B.D. Iverson, *Review of high-temperature central receiver designs for concentrating solar power.* Renewable and sustainable energy reviews, 2014. **29**: p. 835-846.
19. Behar, O., A. Khellaf, and K. Mohammedi, *A review of studies on central receiver solar thermal power plants.* Renewable and Sustainable Energy Reviews, 2013. **23**: p. 12-39.
20. Duffie, J.A. and W.A. Beckman, *Solar engineering of thermal processes*2013: John Wiley & Sons.
21. Dudley, V.E., et al., *Test results: SEGS LS-2 solar collector.* Nasa Sti/recon Technical Report N, 1994. **96**.
22. Eck, M., et al., *Applied research concerning the direct steam generation in parabolic troughs.* Solar Energy, 2003. **74**(4): p. 341-351.
23. Geyer, M., et al. *EUROTROUGH-Parabolic trough collector developed for cost efficient solar power generation*. in *11th International symposium on concentrating solar power and chemical energy technologies*. 2002.
24. Montes, M., et al., *Solar multiple optimization for a solar-only thermal power plant, using oil as heat transfer fluid in the parabolic trough collectors.* Solar Energy, 2009. **83**(12): p. 2165-2176.
25. Liang, H., S. You, and H. Zhang, *Comparison of three optical models and analysis of geometric parameters for parabolic trough solar collectors.* Energy, 2016. **96**: p. 37-47.
26. Garcia, P., A. Ferriere, and J.-J. Bezian, *Codes for solar flux calculation dedicated to central receiver system applications: a comparative review.* Solar Energy, 2008. **82**(3): p. 189-197.
27. Cheng, Z.D., et al., *Numerical simulation of a parabolic trough solar collector with nonuniform solar flux conditions by coupling FVM and MCRT method.* Solar Energy, 2012. **86**(6): p. 1770-1784.
28. Jeter, S.M., *Calculation of the concentrated flux density distribution in parabolic trough collectors by a semifinite formulation.* Solar Energy, 1986. **37**(5): p. 335-345.
29. Grena, R., *Optical simulation of a parabolic solar trough collector.* International Journal of Sustainable Energy, 2010. **29**(1): p. 19-36.
30. Bendt, P., et al., *Optical analysis and optimization of line focus solar collectors*, 1979, Solar Energy Research Inst., Golden, CO (USA).
31. Guven, H. and R. Bannerot, *Derivation of universal error parameters for comprehensive optical analysis of parabolic troughs.* Journal of solar energy engineering, 1986. **108**(4): p. 275-281.
32. Jeter, S.M., *Analytical determination of the optical performance of practical parabolic trough collectors from design data.* Solar Energy, 1987. **39**(1): p. 11-21.
33. Serrano-Aguilera, J.J., L. Valenzuela, and L. Parras, *Thermal 3D model for Direct Solar Steam Generation under superheated conditions.* Applied Energy, 2014. **132**: p. 370-382.
34. He, Y.-L., et al., *A MCRT and FVM coupled simulation method for energy conversion process in parabolic trough solar collector.* Renewable Energy, 2011. **36**(3): p. 976-985.
35. Cheng, Z.D., Y.L. He, and F.Q. Cui, *A new modelling method and unified code with MCRT for concentrating solar collectors and its applications.* Applied Energy, 2013. **101**: p. 686-698.
36. Cheng, Z.D., et al., *Comparative and sensitive analysis for parabolic trough solar collectors with a detailed Monte Carlo ray-tracing optical model.* Applied Energy, 2014. **115**: p. 559-572.
37. Cheng, Z.-D., et al., *A detailed parameter study on the comprehensive characteristics and performance of a parabolic trough solar collector system.* Applied Thermal Engineering, 2014. **63**(1): p. 278-289.
38. Cheng, Z.-D., et al., *Geometric optimization on optical performance of parabolic trough solar collector systems using particle swarm optimization algorithm.* Applied Energy, 2015. **148**: p. 282-293.
39. Hachicha, A.A., et al., *Heat transfer analysis and numerical simulation of a parabolic trough solar collector.* Applied Energy, 2013. **111**: p. 581-592.
40. Hachicha, A.A., I. Rodríguez, and C. Ghenai, *Thermo-hydraulic analysis and numerical simulation of a parabolic trough solar collector for direct steam generation.* Applied Energy, 2018. **214**: p. 152-165.

41. Zou, B., et al., *A detailed study on the optical performance of parabolic trough solar collectors with Monte Carlo Ray Tracing method based on theoretical analysis.* Solar Energy, 2017. **147**: p. 189-201.
42. Liang, H., et al., *A Monte Carlo method and finite volume method coupled optical simulation method for parabolic trough solar collectors.* Applied Energy, 2017. **201**: p. 60-68.
43. Hoseinzadeh, H., A. Kasaeian, and M.B. Shafii, *Geometric optimization of parabolic trough solar collector based on the local concentration ratio using the Monte Carlo method.* Energy Conversion and Management, 2018. **175**: p. 278-287.
44. Wang, F., et al., *Optical efficiency analysis of cylindrical cavity receiver with bottom surface convex.* Solar Energy, 2013. **90**: p. 195-204.
45. Shuai, Y., X.-L. Xia, and H.-P. Tan, *Radiation performance of dish solar concentrator/cavity receiver systems.* Solar Energy, 2008. **82**(1): p. 13-21.
46. Qiu, Y., et al., *A comprehensive model for analysis of real-time optical performance of a solar power tower with a multi-tube cavity receiver.* Applied Energy, 2017. **185**: p. 589-603.
47. Belhomme, B., et al., *A new fast ray tracing tool for high-precision simulation of heliostat fields.* Journal of solar energy engineering, 2009. **131**(3): p. 031002.
48. Jafrancesco, D., et al., *Optical simulation of a central receiver system: Comparison of different software tools.* Renewable and Sustainable Energy Reviews, 2018. **94**: p. 792-803.
49. Noone, C.J., M. Torrilhon, and A. Mitsos, *Heliostat field optimization: A new computationally efficient model and biomimetic layout.* Solar Energy, 2012. **86**(2): p. 792-803.
50. Yao, Z., et al., *Modeling and simulation of the pioneer 1 MW solar thermal central receiver system in China.* Renewable Energy, 2009. **34**(11): p. 2437-2446.
51. Sun, F., et al., *Optical performance of a heliostat in the DAHAN solar power plant.* Energy Procedia, 2014. **49**: p. 239-248.
52. Bode, S.-J. and P. Gauché. *Review of optical software for use in concentrating solar power systems*. in *Proceedings of South African Solar Energy Conference*. 2012.
53. Branke, R. and A. Heimsath, *Raytrace3D power tower—A novel optical model for central receiver systems.* Proceedings of SolarPACES, 2010: p. 21-24.
54. Biggs, F. and C. Vittitoe, *HELIOS: A computational model for solar concentrators.* NASA STI/Recon Technical Report N, 1977. **78**.
55. Leary, P. and J. Hankins, *User's guide for MIRVAL: a computer code for comparing designs of heliostat-receiver optics for central receiver solar power plants*, 1979, Sandia National Laboratories (SNL-CA), Livermore, CA (United States).
56. Monterreal, R. *Software developments for system analysis and optimization*. in *Proceedings of the IEA SolarPACES Task III workshop on simulation of solar thermal power systems*. 2000.
57. Wendelin, T. *SolTRACE: a new optical modeling tool for concentrating solar optics*. in *ASME 2003 International Solar Energy Conference*. 2003. American Society of Mechanical Engineers.
58. Blanco, M.J., J.M. Amieva, and A. Mancillas. *The Tonatiuh Software Development Project: An open source approach to the simulation of solar concentrating systems*. in *ASME 2005 International Mechanical Engineering Congress and Exposition*. 2005. American Society of Mechanical Engineers.
59. Kistler, B.L., *A user's manual for DELSOL3: a computer code for calculating the optical performance and optimal system design for solar thermal central receiver plants.* Sandia National Laboratories, Sandia Report No. SAND86-8018, 1986.
60. Kiera, M., *Beschreibung und handhabung des programmsystems HFLCAL.* Interatom Report, IAS-BT-200000-75, 1986.
61. Sanchez, M. and M. Romero, *Methodology for generation of heliostat field layout in central receiver systems based on yearly normalized energy surfaces.* Solar Energy, 2006. **80**(7): p. 861-874.
62. Osuna, R., et al. *PS10: a 11.0-MW solar tower power plant with saturated steam receiver*. in *Proceedings of the 12th Solar PACES International Symposium on Concentrated Solar Power and Chemical Energy Technologies, Oaxaca, México, October*. 2004.

63. Forristall, R., *Heat transfer analysis and modeling of a parabolic trough solar receiver implemented in engineering equation solver*, 2003, National Renewable Energy Lab., Golden, CO.(US).
64. Clausing, A.M., *An analysis of convective losses from cavity solar central receivers.* Solar Energy, 1981. **27**(4): p. 295-300.
65. Gong, G., et al., *An optimized model and test of the China's first high temperature parabolic trough solar receiver.* Solar Energy, 2010. **84**(12): p. 2230-2245.
66. Rodríguez-Sánchez, M.R., et al., *Comparison of simplified heat transfer models and CFD simulations for molten salt external receiver.* Applied Thermal Engineering, 2014. **73**(1): p. 993-1005.
67. Kalogirou, S.A., *Solar energy engineering: processes and systems*2013: Academic Press.
68. Khanna, S., S.B. Kedare, and S. Singh, *Deflection and stresses in absorber tube of solar parabolic trough due to circumferential and axial flux variations on absorber tube supported at multiple points.* Solar Energy, 2014. **99**: p. 134-151.
69. Khanna, S., S. Singh, and S.B. Kedare, *Explicit expressions for temperature distribution and deflection in absorber tube of solar parabolic trough concentrator.* Solar Energy, 2015. **114**: p. 289-302.
70. García-Valladares, O. and N. Velázquez, *Numerical simulation of parabolic trough solar collector: Improvement using counter flow concentric circular heat exchangers.* International Journal of Heat and Mass Transfer, 2009. **52**(3): p. 597-609.
71. Padilla, R.V., et al., *Heat transfer analysis of parabolic trough solar receiver.* Applied Energy, 2011. **88**(12): p. 5097-5110.
72. Kalogirou, S.A., *A detailed thermal model of a parabolic trough collector receiver.* Energy, 2012. **48**(1): p. 298-306.
73. Yılmaz, İ.H. and M.S. Söylemez, *Thermo-mathematical modeling of parabolic trough collector.* Energy Conversion and Management, 2014. **88**: p. 768-784.
74. Liang, H., S. You, and H. Zhang, *Comparison of different heat transfer models for parabolic trough solar collectors.* Applied Energy, 2015. **148**: p. 105-114.
75. Behar, O., A. Khellaf, and K. Mohammedi, *A novel parabolic trough solar collector model – Validation with experimental data and comparison to Engineering Equation Solver (EES).* Energy Conversion and Management, 2015. **106**: p. 268-281.
76. Tao, Y.B. and Y.L. He, *Numerical study on coupled fluid flow and heat transfer process in parabolic trough solar collector tube.* Solar Energy, 2010. **84**(10): p. 1863-1872.
77. Lu, J., et al., *Nonuniform heat transfer model and performance of parabolic trough solar receiver.* Energy, 2013. **59**: p. 666-675.
78. Cheng, Z.-D., Y.-L. He, and Y. Qiu, *A detailed nonuniform thermal model of a parabolic trough solar receiver with two halves and two inactive ends.* Renewable Energy, 2015. **74**: p. 139-147.
79. Wang, P., et al., *Conjugate heat transfer modeling and asymmetric characteristic analysis of the heat collecting element for a parabolic trough collector.* International Journal of Thermal Sciences, 2016. **101**: p. 68-84.
80. Cengel, Y.A. and A. Ghajar, *Heat and mass transfer (a practical approach, SI version)*, 2011, McGraw-Hill Education.
81. Modest, M.F., *Radiative heat transfer*2013: Academic press.
82. Benoit, H., et al., *Review of heat transfer fluids in tube-receivers used in concentrating solar thermal systems: Properties and heat transfer coefficients.* Renewable and Sustainable Energy Reviews, 2016. **55**: p. 298-315.
83. Gnielinski, V., *New equations for heat and mass transfer in turbulent pipe and channel flow.* Int. Chem. Eng., 1976. **16**(2): p. 359-368.
84. Sandeep, H. and U. Arunachala, *Solar parabolic trough collectors: A review on heat transfer augmentation techniques.* Renewable and Sustainable Energy Reviews, 2017. **69**: p. 1218-1231.
85. Hachicha, A.A., et al., *Numerical simulation of wind flow around a parabolic trough solar collector.* Applied Energy, 2013. **107**: p. 426-437.

86. Odeh, S., M. Behnia, and G. Morrison, *Hydrodynamic analysis of direct steam generation solar collectors.* Journal of Solar Energy Engineering, 2000. **122**(1): p. 14-22.
87. Taitel, Y. and A. Dukler, *A model for predicting flow regime transitions in horizontal and near horizontal gas-liquid flow.* AIChE journal, 1976. **22**(1): p. 47-55.
88. Odeh, S.D., G.L. Morrison, and M. Behnia, *Modelling of parabolic trough direct steam generation solar collectors.* Solar Energy, 1998. **62**(6): p. 395-406.
89. Elsafi, A.M., *On thermo-hydraulic modeling of direct steam generation.* Solar Energy, 2015. **120**: p. 636-650.
90. Pitot de la Beaujardiere, J.-F.P. and H.C.R. Reuter, *A review of performance modelling studies associated with open volumetric receiver CSP plant technology.* Renewable and Sustainable Energy Reviews, 2018. **82**: p. 3848-3862.
91. Harris, J.A. and T.G. Lenz, *Thermal performance of solar concentrator/cavity receiver systems.* Solar Energy, 1985. **34**(2): p. 135-142.
92. Li, X., et al., *Thermal model and thermodynamic performance of molten salt cavity receiver.* Renewable Energy, 2010. **35**(5): p. 981-988.
93. Kribus, A., H. Ries, and W. Spirkl, *Inherent limitations of volumetric solar receivers.* Journal of Solar Energy Engineering, 1996. **118**: p. 151.
94. Bai, F., *One dimensional thermal analysis of silicon carbide ceramic foam used for solar air receiver.* International Journal of Thermal Sciences, 2010. **49**(12): p. 2400-2404.
95. Cheng, Z., et al., *Three-dimensional numerical study of heat transfer characteristics in the receiver tube of parabolic trough solar collector.* International Communications in Heat and Mass Transfer, 2010. **37**(7): p. 782-787.
96. Roldán, M.I., L. Valenzuela, and E. Zarza, *Thermal analysis of solar receiver pipes with superheated steam.* Applied Energy, 2013. **103**: p. 73-84.
97. Li, Z.-Y., Z. Huang, and W.-Q. Tao, *Three-dimensional numerical study on fully-developed mixed laminar convection in parabolic trough solar receiver tube.* Energy, 2016. **113**: p. 1288-1303.
98. Huang, Z., Z.-Y. Li, and W.-Q. Tao, *Numerical study on combined natural and forced convection in the fully-developed turbulent region for a horizontal circular tube heated by non-uniform heat flux.* Applied Energy, 2017. **185**: p. 2194-2208.
99. Qiu, Y., et al., *Thermal performance analysis of a parabolic trough solar collector using supercritical CO2 as heat transfer fluid under non-uniform solar flux.* Applied Thermal Engineering, 2017. **115**: p. 1255-1265.
100. Wang, Y., et al., *Performance analysis of a parabolic trough solar collector with non-uniform solar flux conditions.* International Journal of Heat and Mass Transfer, 2015. **82**: p. 236-249.
101. Lobón, D.H., et al., *Modeling direct steam generation in solar collectors with multiphase CFD.* Applied Energy, 2014. **113**: p. 1338-1348.
102. Lobón, D.H., L. Valenzuela, and E. Baglietto, *Modeling the dynamics of the multiphase fluid in the parabolic-trough solar steam generating systems.* Energy Conversion and Management, 2014. **78**: p. 393-404.
103. Wang, P., D.Y. Liu, and C. Xu, *Numerical study of heat transfer enhancement in the receiver tube of direct steam generation with parabolic trough by inserting metal foams.* Applied Energy, 2013. **102**: p. 449-460.
104. Muñoz, J. and A. Abánades, *Analysis of internal helically finned tubes for parabolic trough design by CFD tools.* Applied Energy, 2011. **88**(11): p. 4139-4149.
105. Mwesigye, A., T. Bello-Ochende, and J.P. Meyer, *Heat transfer and thermodynamic performance of a parabolic trough receiver with centrally placed perforated plate inserts.* Applied Energy, 2014. **136**: p. 989-1003.
106. Fuqiang, W., et al., *Parabolic trough receiver with corrugated tube for improving heat transfer and thermal deformation characteristics.* Applied Energy, 2016. **164**: p. 411-424.
107. Ghadirijafarbeigloo, S., A.H. Zamzamian, and M. Yaghoubi, *3-D Numerical Simulation of Heat Transfer and Turbulent Flow in a Receiver Tube of Solar Parabolic Trough Concentrator with Louvered Twisted-tape Inserts.* Energy Procedia, 2014. **49**: p. 373-380.

108. Naeeni, N. and M. Yaghoubi, *Analysis of wind flow around a parabolic collector (1) fluid flow.* Renewable Energy, 2007. **32**(11): p. 1898-1916.
109. Naeeni, N. and M. Yaghoubi, *Analysis of wind flow around a parabolic collector (2) heat transfer from receiver tube.* Renewable Energy, 2007. **32**(8): p. 1259-1272.
110. Paetzold, J., et al., *Wind engineering analysis of parabolic trough solar collectors: The effects of varying the trough depth.* Journal of Wind Engineering and Industrial Aerodynamics, 2014. **135**: p. 118-128.
111. Paetzold, J., et al., *Wind Engineering Analysis of Parabolic Trough Collectors to Optimise Wind Loads and Heat Loss.* Energy Procedia, 2015. **69**: p. 168-177.
112. Hachicha, A.A., et al., *On the CFD&HT of the Flow around a Parabolic Trough Solar Collector under Real Working Conditions.* Energy Procedia, 2014. **49**: p. 1379-1390.
113. Hachicha, A.A., I. Rodríguez, and A. Oliva, *Wind speed effect on the flow field and heat transfer around a parabolic trough solar collector.* Applied Energy, 2014. **130**: p. 200-211.
114. Mier-Torrecilla, M., E. Herrera, and M. Doblaré, *Numerical Calculation of Wind Loads over Solar Collectors.* Energy Procedia, 2014. **49**: p. 163-173.
115. Andre, M., M. Mier-Torrecilla, and R. Wüchner, *Numerical simulation of wind loads on a parabolic trough solar collector using lattice Boltzmann and finite element methods.* Journal of Wind Engineering and Industrial Aerodynamics, 2015. **146**: p. 185-194.
116. Prakash, M., S.B. Kedare, and J.K. Nayak, *Investigations on heat losses from a solar cavity receiver.* Solar Energy, 2009. **83**(2): p. 157-170.
117. Yang, X., et al., *Numerical simulation study on the heat transfer characteristics of the tube receiver of the solar thermal power tower.* Applied Energy, 2012. **90**(1): p. 142-147.
118. Zheng, Z.-J., M.-J. Li, and Y.-L. He, *Thermal analysis of solar central receiver tube with porous inserts and non-uniform heat flux.* Applied Energy, 2017. **185**: p. 1152-1161.
119. Garbrecht, O., et al., *CFD-simulation of a new receiver design for a molten salt solar power tower.* Solar Energy, 2013. **90**: p. 94-106.
120. Roldán, M. and J. Fernández-Reche. *CFD analysis of supercritical CO2 used as HTF in a solar tower receiver*. in *AIP Conference Proceedings*. 2016. AIP Publishing.
121. Mahmoudi, Y., *Effect of thermal radiation on temperature differential in a porous medium under local thermal non-equilibrium condition.* International Journal of Heat and Mass Transfer, 2014. **76**: p. 105-121.
122. Xu, C., et al., *Numerical investigation on porous media heat transfer in a solar tower receiver.* Renewable Energy, 2011. **36**(3): p. 1138-1144.
123. Wu, Z., et al., *Coupled radiation and flow modeling in ceramic foam volumetric solar air receivers.* Solar Energy, 2011. **85**(9): p. 2374-2385.
124. Wang, P., K. Vafai, and D. Liu, *Analysis of radiative effect under local thermal non-equilibrium conditions in porous media-application to a solar air receiver.* Numerical Heat Transfer, Part A: Applications, 2014. **65**(10): p. 931-948.
125. Roldán, M.I., et al., *Thermal analysis and design of a volumetric solar absorber depending on the porosity.* Renewable Energy, 2014. **62**: p. 116-128.
126. Chen, X., et al., *Thermal performance analysis on a volumetric solar receiver with double-layer ceramic foam.* Energy Conversion and Management, 2015. **97**: p. 282-289.
127. Meng, X.-l., et al., *Coupled heat transfer performance of a high temperature cup shaped porous absorber.* Energy Conversion and Management, 2016. **110**: p. 327-337.
128. Ho, C.K., *A review of high-temperature particle receivers for concentrating solar power.* Applied Thermal Engineering, 2016. **109**: p. 958-969.
129. Meier, A., *A predictive CFD model for a falling particle receiver/reactor exposed to concentrated sunlight.* Chemical Engineering Science, 1999. **54**(13-14): p. 2899-2905.
130. Chen, H., et al. *CFD modeling of gas particle flow within a solid particle solar receiver*. in *ASME 2006 International Solar Energy Conference*. 2006. American Society of Mechanical Engineers.

131. Lee, T., et al., *Numerical simulation of particulate flow in interconnected porous media for central particle-heating receiver applications.* Solar Energy, 2015. **113**: p. 14-24.
132. Martinek, J. and Z. Ma, *Granular flow and heat-transfer study in a near-blackbody enclosed particle receiver.* Journal of Solar Energy Engineering, 2015. **137**(5): p. 051008.
133. Morris, A.B., et al., *Simulations of heat transfer to solid particles flowing through an array of heated tubes.* Solar Energy, 2016. **130**: p. 101-115.
134. Wu, S.-Y., et al., *Convection heat loss from cavity receiver in parabolic dish solar thermal power system: A review.* Solar Energy, 2010. **84**(8): p. 1342-1355.
135. Sezai, I. and A. Mohamad, *Three-dimensional simulation of natural convection in cavities with side opening.* International Journal of Numerical Methods for Heat & Fluid Flow, 1998. **8**(7): p. 800-813.
136. Juárez, J.O., et al., *Numerical study of natural convection in an open cavity considering temperature-dependent fluid properties.* International Journal of Thermal Sciences, 2011. **50**(11): p. 2184-2197.
137. Mohamad, A.A., M. El-Ganaoui, and R. Bennacer, *Lattice Boltzmann simulation of natural convection in an open ended cavity.* International Journal of Thermal Sciences, 2009. **48**(10): p. 1870-1875.
138. Flesch, R., et al., *On the influence of wind on cavity receivers for solar power towers: An experimental analysis.* Applied Thermal Engineering, 2015. **87**: p. 724-735.
139. Xiao, L., S.-Y. Wu, and Y.-R. Li, *Numerical study on combined free-forced convection heat loss of solar cavity receiver under wind environments.* International Journal of Thermal Sciences, 2012. **60**: p. 182-194.
140. Hu, T., et al., *Numerical simulation on convective thermal loss of a cavity receiver in a solar tower power plant.* Solar Energy, 2017. **150**: p. 202-211.
141. Roldán, M.I., J. Fernández-Reche, and J. Ballestrín, *Computational fluid dynamics evaluation of the operating conditions for a volumetric receiver installed in a solar tower.* Energy, 2016. **94**: p. 844-856.
142. Marais, M.D., K.J. Craig, and J.P. Meyer, *Computational Flow Optimization of Heliostat Aspect Ratio for Wind Direction and Elevation Angle.* Energy Procedia, 2015. **69**: p. 148-157.
143. Wu, Z. and Z. Wang, *Numerical study of wind load on heliostat.* Progress in Computational Fluid Dynamics, an International Journal, 2008. **8**(7-8): p. 503-509.
144. Shademan, M., R. Balachandar, and R.M. Barron, *Detached eddy simulation of flow past an isolated inclined solar panel.* Journal of Fluids and Structures, 2014. **50**: p. 217-230.
145. Boddupalli, N., V. Goenka, and L. Chandra. *Fluid flow analysis behind heliostat using LES and RANS: A step towards optimized field design in desert regions*. in *AIP Conference Proceedings*. 2017. AIP Publishing.
146. Boddupalli, N., et al., *Dealing with dust – Some challenges and solutions for enabling solar energy in desert regions.* Solar Energy, 2017. **150**: p. 166-176.
147. Xu, L., et al., *Dynamic test model for the transient thermal performance of parabolic trough solar collectors.* Solar Energy, 2013. **95**: p. 65-78.
148. Ho, C.K., *Software and codes for analysis of concentrating solar power technologies*, 2008, Sandia National Laboratories.
149. Liang, H., et al., *Analysis of Annual Performance of a Parabolic Trough Solar Collector.* Energy Procedia, 2017. **105**: p. 888-894.
150. Marif, Y., et al., *Numerical simulation of solar parabolic trough collector performance in the Algeria Saharan region.* Energy Conversion and Management, 2014. **85**: p. 521-529.
151. Kumar, D. and S. Kumar, *Year-round performance assessment of a solar parabolic trough collector under climatic condition of Bhiwani, India: A case study.* Energy Conversion and Management, 2015. **106**: p. 224-234.
152. Yang, S., T.S. Sensoy, and J.C. Ordonez, *Dynamic 3D volume element model of a parabolic trough solar collector for simulation and optimization.* Applied Energy, 2018. **217**: p. 509-526.
153. You, C., W. Zhang, and Z. Yin, *Modeling of fluid flow and heat transfer in a trough solar collector.* Applied Thermal Engineering, 2013. **54**(1): p. 247-254.
154. Yan, Q., et al., *Dynamic modeling and simulation of a solar direct steam-generating system.* International Journal of Energy Research, 2010. **34**(15): p. 1341-1355.

155. Patnode, A.M., *Simulation and performance evaluation of parabolic trough solar power plants*, 2006, University of Wisconsin--Madison.
156. Montañés, R.M., et al., *Dynamic Modeling of a Parabolic Trough Solar Thermal Power Plant with Thermal Storage Using Modelica.* Heat Transfer Engineering, 2018. **39**(3): p. 277-292.
157. Wagner, M.J., N. Blair, and A. Dobos, *Detailed Physical Trough Model for NREL's Solar Advisor Model: Preprint*, 2010, National Renewable Energy Lab.(NREL), Golden, CO (United States).
158. Yu, Q., Z. Wang, and E. Xu, *Simulation and analysis of the central cavity receiver's performance of solar thermal power tower plant.* Solar Energy, 2012. **86**(1): p. 164-174.
159. Ferriere, A., B. Bonduelle, and M. Amouroux, *Development of an Optimal Control Strategy for the Themis Solar Plant: Part I—Themis Transient Model.* Journal of Solar Energy Engineering, 1989. **111**(4): p. 298-304.
160. Zhang, Q., et al., *Modeling and simulation of a molten salt cavity receiver with Dymola.* Energy, 2015. **93**: p. 1373-1384.
161. Xu, E., et al., *Modeling and simulation of 1 MW DAHAN solar thermal power tower plant.* Renewable Energy, 2011. **36**(2): p. 848-857.
162. Yao, Z., et al., *Modeling and simulation of the pioneer 1MW solar thermal central receiver system in China.* Renewable Energy, 2009. **34**(11): p. 2437-2446.
163. Flueckiger, S.M., et al., *System-level simulation of a solar power tower plant with thermocline thermal energy storage.* Applied Energy, 2014. **113**: p. 86-96.
164. Ahlbrink, N., B. Belhomme, and R. Pitz-Paal. *Modeling and simulation of a solar tower power plant with open volumetric air receiver*. in *Proceedings of the 7th International Modelica Conference; Como; Italy; 20-22 September 2009*. 2009. Linköping University Electronic Press.
165. Binotti, M., et al., *Geometric analysis of three-dimensional effects of parabolic trough collectors.* Solar Energy, 2013. **88**: p. 88-96.
166. Hachicha, A.A., I. Al-Sawafta, and D. Ben Hamadou, *Numerical and Experimental Investigations of Dust Effect on CSP Performance under United Arab Emirates Weather Conditions.* Renewable Energy, 2019.
167. Bellos, E. and C. Tzivanidis, *A review of concentrating solar thermal collectors with and without nanofluids.* Journal of Thermal Analysis and Calorimetry, 2019. **135**(1): p. 763-786.
168. Hasanpour, A., M. Farhadi, and K. Sedighi, *A review study on twisted tape inserts on turbulent flow heat exchangers: The overall enhancement ratio criteria.* International Communications in Heat and Mass Transfer, 2014. **55**: p. 53-62.
169. Bellos, E., C. Tzivanidis, and D. Tsimpoukis, *Enhancing the performance of parabolic trough collectors using nanofluids and turbulators.* Renewable and Sustainable Energy Reviews, 2018. **91**: p. 358-375.
170. Bellos, E., I. Daniil, and C. Tzivanidis, *Multiple cylindrical inserts for parabolic trough solar collector.* Applied Thermal Engineering, 2018. **143**: p. 80-89.
171. Mwesigye, A., T. Bello-Ochende, and J.P. Meyer, *Heat transfer and entropy generation in a parabolic trough receiver with wall-detached twisted tape inserts.* International Journal of Thermal Sciences, 2016. **99**: p. 238-257.
172. Jaramillo, O.A., et al., *Parabolic trough solar collector for low enthalpy processes: An analysis of the efficiency enhancement by using twisted tape inserts.* Renewable Energy, 2016. **93**: p. 125-141.
173. Song, X., et al., *A numerical study of parabolic trough receiver with nonuniform heat flux and helical screw-tape inserts.* Energy, 2014. **77**: p. 771-782.
174. Chang, C., et al., *Heat Transfer Enhancement and Performance of Solar Thermal Absorber Tubes with Circumferentially Non-uniform Heat Flux.* Energy Procedia, 2015. **69**: p. 320-327.
175. Zhu, X., L. Zhu, and J. Zhao, *Wavy-tape insert designed for managing highly concentrated solar energy on absorber tube of parabolic trough receiver.* Energy, 2017. **141**: p. 1146-1155.
176. Cheng, Z.D., Y.L. He, and F.Q. Cui, *Numerical study of heat transfer enhancement by unilateral longitudinal vortex generators inside parabolic trough solar receivers.* International Journal of Heat and Mass Transfer, 2012. **55**(21): p. 5631-5641.

177. Huang, Z., et al., *Numerical investigations on fully-developed mixed turbulent convection in dimpled parabolic trough receiver tubes.* Applied Thermal Engineering, 2017. **114**: p. 1287-1299.
178. Fuqiang, W., et al., *Heat transfer performance enhancement and thermal strain restrain of tube receiver for parabolic trough solar collector by using asymmetric outward convex corrugated tube.* Energy, 2016. **114**: p. 275-292.
179. Ebrahim Ghasemi, S. and A. Akbar Ranjbar, *Numerical thermal study on effect of porous rings on performance of solar parabolic trough collector.* Applied Thermal Engineering, 2017. **118**: p. 807-816.
180. Bellos, E., et al., *Thermal enhancement of solar parabolic trough collectors by using nanofluids and converging-diverging absorber tube.* Renewable Energy, 2016. **94**: p. 213-222.
181. Bellos, E., C. Tzivanidis, and D. Tsimpoukis, *Multi-criteria evaluation of parabolic trough collector with internally finned absorbers.* Applied Energy, 2017. **205**: p. 540-561.
182. Bitam, E.W., et al., *Numerical investigation of a novel sinusoidal tube receiver for parabolic trough technology.* Applied Energy, 2018. **218**: p. 494-510.
183. Şahin, H.M., et al., *Investigation of heat transfer enhancement in a new type heat exchanger using solar parabolic trough systems.* International Journal of Hydrogen Energy, 2015. **40**(44): p. 15254-15266.
184. Soo Too, Y.C. and R. Benito, *Enhancing heat transfer in air tubular absorbers for concentrated solar thermal applications.* Applied Thermal Engineering, 2013. **50**(1): p. 1076-1083.
185. Liao, Z. and A. Faghri, *Thermal analysis of a heat pipe solar central receiver for concentrated solar power tower.* Applied Thermal Engineering, 2016. **102**: p. 952-960.
186. Craig, K.J., M. Slootweg, and J.P. Meyer, *HEAT TRANSFER ENHANCEMENT IN MOLTEN SALT CENTRAL RECEIVER USING JET IMPINGEMENT.*
187. Sarker, M.R.I., S. Mandal, and S.S. Tuly, *Numerical study on the influence of vortex flow and recirculating flow into a solid particle solar receiver.* Renewable Energy, 2018. **129**: p. 409-418.
188. Rodríguez-Sánchez, M.R., et al., *New Designs of Molten-salt Tubular-receiver for Solar Power Tower.* Energy Procedia, 2014. **49**: p. 504-513.
189. Daabo, A.M., S. Mahmoud, and R.K. Al-Dadah, *The optical efficiency of three different geometries of a small scale cavity receiver for concentrated solar applications.* Applied Energy, 2016. **179**: p. 1081-1096.
190. Hischier, I., et al., *Heat transfer analysis of a novel pressurized air receiver for concentrated solar power via combined cycles.* Journal of Thermal Science and Engineering Applications, 2009. **1**(4): p. 041002.
191. Manikandan, G., S. Iniyan, and R. Goic, *Enhancing the optical and thermal efficiency of a parabolic trough collector–A review.* Applied Energy, 2019. **235**: p. 1524-1540.
192. Gupta, M., et al., *A review on thermophysical properties of nanofluids and heat transfer applications.* Renewable and Sustainable Energy Reviews, 2017. **74**: p. 638-670.
193. Javadi, F., R. Saidur, and M. Kamalisarvestani, *Investigating performance improvement of solar collectors by using nanofluids.* Renewable and Sustainable Energy Reviews, 2013. **28**: p. 232-245.
194. Choi, S.U. and J.A. Eastman, *Enhancing thermal conductivity of fluids with nanoparticles*, 1995, Argonne National Lab., IL (United States).
195. Eastman, J., et al., *Enhanced thermal conductivity through the development of nanofluids.* MRS Online Proceedings Library Archive, 1996. **457**.
196. Khanafer, K. and K. Vafai, *A review on the applications of nanofluids in solar energy field.* Renewable Energy, 2018. **123**: p. 398-406.
197. Menbari, A., A.A. Alemrajabi, and A. Rezaei, *Experimental investigation of thermal performance for direct absorption solar parabolic trough collector (DASPTC) based on binary nanofluids.* Experimental Thermal and Fluid Science, 2017. **80**: p. 218-227.
198. Kasaeian, A., et al., *Experimental investigation on the thermal behavior of nanofluid direct absorption in a trough collector.* Journal of Cleaner Production, 2017. **158**: p. 276-284.
199. Xuan, Y. and W. Roetzel, *Conceptions for heat transfer correlation of nanofluids.* International Journal of Heat and Mass Transfer, 2000. **43**(19): p. 3701-3707.

200. Sarkar, J., *A critical review on convective heat transfer correlations of nanofluids.* Renewable and Sustainable Energy Reviews, 2011. **15**(6): p. 3271-3277.
201. Bellos, E. and C. Tzivanidis, *Thermal analysis of parabolic trough collector operating with mono and hybrid nanofluids.* Sustainable Energy Technologies and Assessments, 2018. **26**: p. 105-115.
202. Kasaiean, A., et al., *Heat transfer network for a parabolic trough collector as a heat collecting element using nanofluid.* Renewable Energy, 2018. **123**: p. 439-449.
203. Sokhansefat, T., A.B. Kasaeian, and F. Kowsary, *Heat transfer enhancement in parabolic trough collector tube using Al2O3/synthetic oil nanofluid.* Renewable and Sustainable Energy Reviews, 2014. **33**: p. 636-644.
204. Ghasemi, S.E. and A.A. Ranjbar, *Thermal performance analysis of solar parabolic trough collector using nanofluid as working fluid: A CFD modelling study.* Journal of Molecular Liquids, 2016. **222**: p. 159-166.
205. Ghasemi, S.E. and A.A. Ranjbar, *Effect of using nanofluids on efficiency of parabolic trough collectors in solar thermal electric power plants.* International Journal of Hydrogen Energy, 2017. **42**(34): p. 21626-21634.
206. Mwesigye, A., Z. Huan, and J.P. Meyer, *Thermal performance and entropy generation analysis of a high concentration ratio parabolic trough solar collector with Cu-Therminol®VP-1 nanofluid.* Energy Conversion and Management, 2016. **120**: p. 449-465.
207. Mwesigye, A. and J.P. Meyer, *Optimal thermal and thermodynamic performance of a solar parabolic trough receiver with different nanofluids and at different concentration ratios.* Applied Energy, 2017. **193**: p. 393-413.
208. Mwesigye, A., İ.H. Yılmaz, and J.P. Meyer, *Numerical analysis of the thermal and thermodynamic performance of a parabolic trough solar collector using SWCNTs-Therminol®VP-1 nanofluid.* Renewable Energy, 2018. **119**: p. 844-862.
209. Wang, Y., et al., *Performance analysis of a parabolic trough solar collector using Al2O3/synthetic oil nanofluid.* Applied Thermal Engineering, 2016. **107**: p. 469-478.
210. Kaloudis, E., E. Papanicolaou, and V. Belessiotis, *Numerical simulations of a parabolic trough solar collector with nanofluid using a two-phase model.* Renewable Energy, 2016. **97**: p. 218-229.
211. Minea, A.A. and W.M. El-Maghlany, *Influence of hybrid nanofluids on the performance of parabolic trough collectors in solar thermal systems: Recent findings and numerical comparison.* Renewable Energy, 2018. **120**: p. 350-364.
212. Marefati, M., M. Mehrpooya, and M.B. Shafii, *Optical and thermal analysis of a parabolic trough solar collector for production of thermal energy in different climates in Iran with comparison between the conventional nanofluids.* Journal of Cleaner Production, 2018. **175**: p. 294-313.
213. Allouhi, A., et al., *Energy and exergy analyses of a parabolic trough collector operated with nanofluids for medium and high temperature applications.* Energy Conversion and Management, 2018. **155**: p. 201-217.
214. Khakrah, H., A. Shamloo, and S.K. Hannani, *Determination of parabolic trough solar collector efficiency using nanofluid: a comprehensive numerical study.* Journal of Solar Energy Engineering, 2017. **139**(5): p. 051006.
215. Jin, H., et al., *Steam generation in a nanoparticle-based solar receiver.* Nano Energy, 2016. **28**: p. 397-406.
216. Neumann, O., et al., *Solar vapor generation enabled by nanoparticles.* ACS nano, 2012. **7**(1): p. 42-49.
217. Ni, G., et al., *Volumetric solar heating of nanofluids for direct vapor generation.* Nano Energy, 2015. **17**: p. 290-301.
218. Otanicar, T.P., P.E. Phelan, and J.S. Golden, *Optical properties of liquids for direct absorption solar thermal energy systems.* Solar Energy, 2009. **83**(7): p. 969-977.
219. Slocum, A.H., et al., *Concentrated solar power on demand.* Solar Energy, 2011. **85**(7): p. 1519-1529.
220. Miller, F.J. and R.W. Koenigsdorff, *Thermal modeling of a small-particle solar central receiver.* Journal of Solar Energy Engineering, 2000. **122**(1): p. 23-29.
221. Said, Z., et al., *Acid-functionalized carbon nanofibers for high stability, thermoelectrical and electrochemical properties of nanofluids.* Journal of colloid and interface science, 2018. **520**: p. 50-57.
222. Zhu, D., et al., *Intriguingly high thermal conductivity increment for CuO nanowires contained nanofluids with low viscosity.* Scientific reports, 2018. **8**(1): p. 5282.

223. Oman, J. and P. Novak, *Volumetric absorption in gas—properties of particles and particle-gas suspensions.* Solar Energy, 1996. **56**(6): p. 597-606.
224. Bohn, M. and K. Wang, *Experiments and analysis on the molten Salt direct absorption receiver concept.* Journal of Solar Energy Engineering, 1988. **110**(1): p. 45-51.
225. Veeraragavan, A., et al., *Analytical model for the design of volumetric solar flow receivers.* International journal of heat and mass transfer, 2012. **55**(4): p. 556-564.
226. Kumar, S. and C. Tien, *Analysis of combined radiation and convection in a particulate-laden liquid film.* Journal of solar energy engineering, 1990. **112**(4): p. 293-300.
227. Miller, F. and R. Koenigsdorff, *Theoretical analysis of a high-temperature small-particle solar receiver.* Solar Energy Materials, 1991. **24**(1-4): p. 210-221.
228. Taylor, R.A., et al., *Applicability of nanofluids in high flux solar collectors.* Journal of Renewable and Sustainable Energy, 2011. **3**(2): p. 023104.
229. Sarker, M.R.I., et al., *Recirculating metallic particles for the efficiency enhancement of concentrated solar receivers.* Renewable Energy, 2016. **96**: p. 850-862.
230. Liu, J., et al., *A combined numerical and experimental study on graphene/ionic liquid nanofluid based direct absorption solar collector.* Solar Energy Materials and Solar Cells, 2015. **136**: p. 177-186.
231. Lenert, A. and E.N. Wang, *Optimization of nanofluid volumetric receivers for solar thermal energy conversion.* Solar Energy, 2012. **86**(1): p. 253-265.